

# Ab Initio Study of Lower Energy Phenol–Water<sub>1≤n≤4</sub> Complexes: Interpretation of Two Distinct Infrared Patterns in Spectra of Phenol–Water Tetramer<sup>†</sup>

Eugene S. Kryachko<sup>\*,‡</sup> and Hiroshi Nakatsuji<sup>§</sup>

Department of Chemistry, University of Leuven, Celestijnenlaan 200F, B-3001 Leuven, Belgium, and  
Department of Synthetic Chemistry and Biological Chemistry, Graduate School of Engineering,  
Kyoto University, Kyoto 606, Japan

Received: June 11, 2001; In Final Form: October 20, 2001

The lower energy portion of the potential energy surface of the interaction between phenol and four water molecules is thoroughly studied at a variety of computational levels including HF, MP2, and B3LYP in conjunction with 6-31G(d) basis set and MP2/6-31+G(d). The aim of the present work is 2-fold: first, to juxtapose this potential energy surface with those of the phenol–water<sub>n=1–3</sub> complexes, whose bottoms are occupied by the structures exhibiting 2D ring-type arrangement of water molecules, and second, to offer a new sound theoretical interpretation of the experimental results obtained by the Stanley and Castleman and by the Mikami and Ebata groups via demonstrating a firm existence of the lower energy phenol–water<sub>4</sub> isomer characterized by a *three-dimensional* arrangement of its water molecules. We show that it is precisely that isomer which is capable to provide a complete explanation of the puzzled “window” region in the IR stretching spectra of the phenol–water<sub>4</sub> complex. Its three-dimensionality originates due that one of its water molecules form a  $\pi$  hydrogen bond with  $\pi$  cloud of the phenol ring. We explain a sort of “magic” of the number *four* of water molecules interacting with phenol in terms of that the ability of the phenolic OH-group to accept a hydrogen bond from water molecule becomes nearly exhausted when *three* water molecules form a *two-dimensional* ring and, therefore, competes with the ability of the  $\pi$  cloud of the phenol ring to form a  $\pi$  hydrogen bonding leading to a *three-dimensional* pattern.

## 1. Introduction

A knowledge of the potential energy surface (PES) of a molecular complex is always a key goal in study of its vibrational pattern and dynamics. The PES of interaction of water clusters with phenol (designated herein as Ph) is rather particular for several reasons. The prime reason is that phenol–water complexes are formed via hydrogen (H-) bonds and can thus be treated as prototypes for hydrogen-bonded aromatic systems and models of diverse important chemical and biological processes, such as, e.g., solute–solvent interactions involving a participation of hydrogen bonds.

Hydrogen-bonded phenol–water complexes Ph(H<sub>2</sub>O)<sub>n</sub> (Ph–w<sub>n</sub>) have been thoroughly studied experimentally<sup>1–10</sup> by standard spectroscopic methods, in particular, by laser-induced fluorescence, resonance-enhanced multiphoton ionization, high-resolution UV spectroscopy, single vibronic level dispersed fluorescence, and hole-burning spectroscopy. The mass-selected multiphoton ionization study of these complexes with  $n \leq 4$  were first conducted by Lipert and Colson<sup>2</sup> who argued that the ground-state global minimum structure of Ph(H<sub>2</sub>O)<sub>2</sub> is realized when water molecules form a ring S<sub>2</sub> (see also refs 1–5). Comparing the spectra of the Ph(H<sub>2</sub>O)<sub>1–3</sub> complexes, Lipert and Colson were led to the conclusion that these three complexes should not be treated as a sequence of additive

derivatives and, moreover, they might even have different geometries. The two-color photoionization and cluster ion dip spectroscopy of Ph(H<sub>2</sub>O)<sub>n≤4</sub> were carried out by Stanley and Castleman<sup>7</sup> who particularly admitted the existence of two isomers of Ph(H<sub>2</sub>O)<sub>4</sub>. The Raman spectrum of Ph(H<sub>2</sub>O)<sub>1</sub> was also observed by Hartland et al.<sup>3</sup>

The infrared (IR) and Raman UV double-resonance spectroscopy of Ph(H<sub>2</sub>O)<sub>n≤4</sub> in the OH stretching vibration region were studied by Ebata et al.,<sup>6a</sup> Tanabe et al.,<sup>6b</sup> Mikami,<sup>6c</sup> and Watanabe et al.<sup>6d</sup> They concluded that, on one hand, the symmetric water  $\nu_1$  and phenolic OH stretching ( $\nu_{OH}$ ) vibrations are considerably downshifted under the formation of phenol–water complexes compared with those inherent for bare water and phenol molecules. On the other hand, the antisymmetric  $\nu_3$  vibration of water molecule is weakly affected. This develops in the appearance of a transparent “window” region<sup>6c</sup> in the IR spectrum of Ph(H<sub>2</sub>O)<sub>n=2–4</sub> which widens as  $n$  increases, having a width of ca. 280 cm<sup>-1</sup> for  $n = 4$ , and disappears in the spectrum of the Ph(H<sub>2</sub>O)<sub>5</sub> complex.<sup>5b</sup> Mikami<sup>6c</sup> explained the origin of the “window” region by the presence of the cyclic S<sub>n</sub> arrangements of water molecules in these complexes with  $n \leq 4$ . Interestingly, these authors also observed a completely different IR pattern for Ph(H<sub>2</sub>O)<sub>4</sub> in the region of the OH stretching vibrations where four bands fall into this “window” region.<sup>6c–d</sup> It has then been particularly suggested that such pattern is due to the second isomer of Ph(H<sub>2</sub>O)<sub>4</sub> which was observed by Stanley and Castleman<sup>7a</sup> and which might have a substantially different structure of water molecules compared to the cyclic one or even a mixture of different isomers.<sup>6d</sup> Jacoby et al.<sup>4d</sup> have recently performed the resonant two-photon ionization study of Ph(H<sub>2</sub>O)<sub>2–5</sub> and Ph(D<sub>2</sub>O)<sub>2–5-d1</sub> complexes

<sup>†</sup> Dedicated to the 70th birthday of Georg Zundel.

<sup>\*</sup> Corresponding author. Phone: +32 (16) 32 73 84. FAX: +32 (16) 32 79 92. E-mail: eugene@hartree.chem.kuleuven.ac.be. On leave from Bogoliubov Institute for Theoretical Physics, Kiev, 03143 Ukraine. E-mail: eugen@gluk.or.

<sup>‡</sup> Department of Chemistry.

<sup>§</sup> Department of Synthetic Chemistry and Biological.

and came to the conclusion that this second isomer of  $\text{Ph}(\text{H}_2\text{O})_4$  may be characterized by a noncyclic, more compact water arrangement. Such arrangement can be only expected for cage-, prism-, boat-, and book-like structures of water clusters (for the nomenclature of water clusters structures, see, e.g., ref 11 and references therein) around phenol similar to the book-like structure of water molecules in the global-minimum  $\text{Ph}(\text{H}_2\text{O})_5$  complex where one water molecule forms an anchor-type  $\pi$  H-bond with the aromatic ring.<sup>5b,5d</sup> Altogether, this briefly outlines the experimental facet of the current state of art of the phenol–water interaction. Its theoretical one is the following.

The first ab initio calculations of  $\text{Ph}(\text{H}_2\text{O})_1$  were performed by Gerhards et al.<sup>5a</sup> and Schmitt et al.<sup>5c</sup> at the Hartree–Fock (HF) level and by Feller and Feyereisen<sup>12</sup> at the second-order correlated Møller–Plessett (MP2) level with 6-31G(d,p) basis set within a frozen core (fc) approximation (for recent studies see refs 13 and 14). Density functional B3LYP calculation of  $\text{Ph}(\text{H}_2\text{O})_n$  have been recently carried out by Sodupe et al.<sup>15a</sup> and Guedes et al.<sup>15b</sup> The ground-state  $\text{Ph}(\text{H}_2\text{O})_2$  complex was first optimized by Leutwyler et al.<sup>8d</sup> and Gerhards and Kleinermanns<sup>4c</sup> (see also refs 13b,c, 15b, and 16). The structure and vibrations of  $\text{Ph}(\text{H}_2\text{O})_3$  in the singlet ground and its first excited state, and the lowest triplet state were investigated by Bürgi et al.<sup>8e</sup> and Schmitt et al.<sup>4a</sup> at the HF/6-31G(d,p) computational level. Bürgi et al.<sup>8e</sup> also reported several local minima on the ground-state PES of  $\text{Ph}(\text{H}_2\text{O})_3$  lying 8–14 kcal/mol above the global-minimum structure with the cyclic  $S_3$  water arrangement.

Based on the theoretical study of the  $\text{Ph}(\text{H}_2\text{O})_n$  complexes calculated preliminarily at the HF/6-31G(d) computational level and further refined at the MP2(fc)/6-31G one, Watanabe and Iwata<sup>17a</sup> concluded that the “window” region originates from the spectra of the  $\text{Ph}(\text{H}_2\text{O})_4$  isomer with the cyclic water structure  $S_4$ . Another, experimentally observed IR pattern of  $\text{Ph}(\text{H}_2\text{O})_4$  does not fit the theoretical spectra of any complex found in their study and may likely be attributed to a mixture of some complexes characterized by more compact water arrangements. The proton-transfer  $\text{Ph}(\text{H}_2\text{O})_4$  complex suggested by Mikami<sup>6c</sup> and Watanabe et al.<sup>6d</sup> as a possible candidate for the second isomer was declined by Watanabe and Iwata<sup>17b</sup> (see also ref 4d). This clearly demonstrates that the origin of the second isomer revealed experimentally by Stanley and Castleman<sup>7a</sup> and its contribution to the substantially different IR pattern still remain an unsolved problem.

The aim of the present work consists of performing a rather thorough search of the ground-state PES of the  $\text{Ph}(\text{H}_2\text{O})_{n=3,4}$  complexes in the vicinity of the global minimum in order to reveal its lower energy minimum structures and to offer a new sound explanation of the origin of two different “window” patterns in the IR spectra of the  $\text{Ph}(\text{H}_2\text{O})_4$  complex. Actually, a “window” region measures a strength of hydrogen bonding: the larger the “window”, the stronger the bonding (see also ref 18). In the present work, we also use a canonical rationale to evaluate a strength of hydrogen bonding in terms of the corresponding stretching vibration  $\nu_\sigma$  of H-bond bridge.<sup>19</sup> Notice that a blue-shifted torsion vibration  $\tau_{\text{OH}}$  of phenol can be employed for this purpose as well.

The remainder of the present work has the following layout. At the outset, section 2 outlines the computational methodology and summarizes some calculated properties of the isolated phenol and water molecules as the reference ones essential for a further discussion. Section 3 is composed of three Subsections. Subsection 3.A briefly reports two most lower energy structures of  $\text{Ph}(\text{H}_2\text{O})_{n=1,2}$  and their theoretical spectra while section 3.B

demonstrates the existence of three lower energy structures on the PES of  $\text{Ph}(\text{H}_2\text{O})_3$  lying by less than 3 kcal/mol above the global minimum. This, on one hand, shows a relative richness of the landscape of the PES of  $\text{Ph}(\text{H}_2\text{O})_3$  in comparison with the PES reported by Bürgi et al.<sup>8e</sup> and the three structures found by Watanabe and Iwata<sup>17a</sup> at the same computational level and located within 6.64 kcal/mol above its bottom. On the other one, we also reveal a novel structure where one of the water molecules forms a so-called  $\pi$  hydrogen bond with  $\pi$  electrons of the phenol ring. It partly resembles the analogous structure named Leg2 and found for the benzene–water complex (see ref 20 for current review). Section 3.C is actually the key part of the present work. It deals with 10 lower energy local minimum structures of the  $\text{Ph}(\text{H}_2\text{O})_4$  complex compared with the five ones reported in ref 17a and located within nearly the same interval of energies, ca. 3.81 kcal/mol, above the global energy minimum. In this section we propose a new interpretation of the Mikami and Ebata group<sup>6c–d</sup> experiments on the existence of two different patterns in the IR spectra of  $\text{Ph}(\text{H}_2\text{O})_4$  and confirm the observation by Stanley and Castleman.<sup>7a</sup> The essential conclusions of the present work are embodied in section 4.

## 2. Computational Methodology

By the analogy with the earlier studies,<sup>17</sup> the PES search of the phenol–water<sub>*n*</sub> complexes was initially performed by using a split-valence double- $\zeta$  6-31G(d) basis set<sup>21</sup> via GAUSSIAN 98 suit of packages.<sup>22</sup> For the reasons which will be explained in the next sections, we distinguish five computational levels of theory/basis sets used for geometry optimizations although a 6-31G(d) basis set denoted throughout the present work as A plays a key role. The ground level corresponds to the common HF/A one which is also employed to calculate harmonic vibrational frequencies, zero-point vibrational energy (ZPVE), and thermodynamic properties. Empirical scaling factor of 0.8907 introduced in ref 17a was not used in the present work. Single-point (sp) energy calculations of the lower energy  $\text{Ph}(\text{H}_2\text{O})_n$  complexes were further performed at the MP2(sp)/A level aimed to investigate the effect of correlation on their energy differences. The most stable  $\text{Ph}(\text{H}_2\text{O})_{1 \leq n \leq 4}$  structures as the key structures in the present study were further refined at the MP2(fc)/A (fc is hereafter omitted). The four lowest energy structures  $\text{Ph}(\text{H}_2\text{O})_4$  structures were also reoptimized at the MP2/6-31+G(d) ( $\equiv$  MP2/A<sup>+</sup>) and B3LYP/A levels. The latter was also used to recalculate their harmonic frequencies.

In the present study, phenol and  $\text{H}_2\text{O}$  play a role of the reference molecules. The chosen computational methods accurately describe properties of phenol, particularly its vibrational spectrum.<sup>23</sup> The frequencies of the OH stretching vibrations of phenol and water molecule are collected in Table 1. It is then interesting to note that the HF/A frequency of 4118  $\text{cm}^{-1}$  assigned to the  $\nu_{\text{OH}}$  stretching vibration of bare phenol corresponds to its most accepting mode.  $\nu_{\text{OH}}$  lies between the  $\nu_1$  (4070  $\text{cm}^{-1}$ ) and  $\nu_3$  (4188  $\text{cm}^{-1}$ ) OH stretching vibrational modes of water molecule, viz.,

$$\nu_1 < \overset{48}{\nu_{\text{OH}}} < \overset{70}{\nu_3} \quad (1)$$

Here a value above the inequality sign indicates the corresponding frequency difference in  $\text{cm}^{-1}$  between its left- and right-hand side quantities. It follows from eq 1 that the first difference  $\Delta\nu = \nu_{\text{OH}} - \nu_1$  is equal to 48  $\text{cm}^{-1}$ .

## 3. Hydration of Phenol

**3.A. The Most Stable Complexes of Mono- and Dihydrated Phenol.** Phenol is certainly more acidic than water, and

**TABLE 1:** The OH Stretch Frequencies, in cm<sup>-1</sup>, of Water and Phenol, and Phenol–Water<sub>1,2</sub> Complexes Calculated via the HF/A and MP2/A (in Parentheses) Computational Methods: Infrared Intensity in km/mol, Raman (R) Activity in Å<sup>4</sup>/amu

	$\nu_1$			$\nu_3$			$\nu_{OH}$			
	freq	IR	R	freq	IR	R	freq	IR	R	
H <sub>2</sub> O	4070.0	3658 <sup>a</sup>	18	4188.2	3756 <sup>a</sup>	58	39			
Ph								4118.1	3657 <sup>b</sup>	81
								4197.2	(3881.8) <sup>c</sup>	84 (53)
Ph-w <sub>1</sub> -1	4068.6 (3764.1)	22 (18)	69	4182.0 (3897.4)	102 (81)	54		4008.9 (3597.8)	537 (645)	144
	3650 <sup>b</sup>			3748 <sup>b</sup>				3524 <sup>b</sup>		
Ph-w <sub>1</sub> -2	4057.2	94	89	4170.2	134	41		4114.3	94	73
Ph-w <sub>2</sub> -1	3973.2 (3560.7)	308 (419)	47	4147.1 (3846.9)	121 (99)	81		3916.6 (3420.9)	393 (501)	156
	4021.7 (3662.7)	237 (282)	58	4154.7 (3850.2)	137 (69)	40				

<sup>a</sup> Experimental frequencies of water are taken from ref 24. <sup>b</sup> Experimental frequencies for phenol and phenol–water clusters are taken from refs 6c,d. See also ref 21 for the phenol vibrational modes. <sup>c</sup> Calculated frequency at the HF/6-31G(d,p) and MP2/6-31G(d,p) (in parentheses) levels 21a.

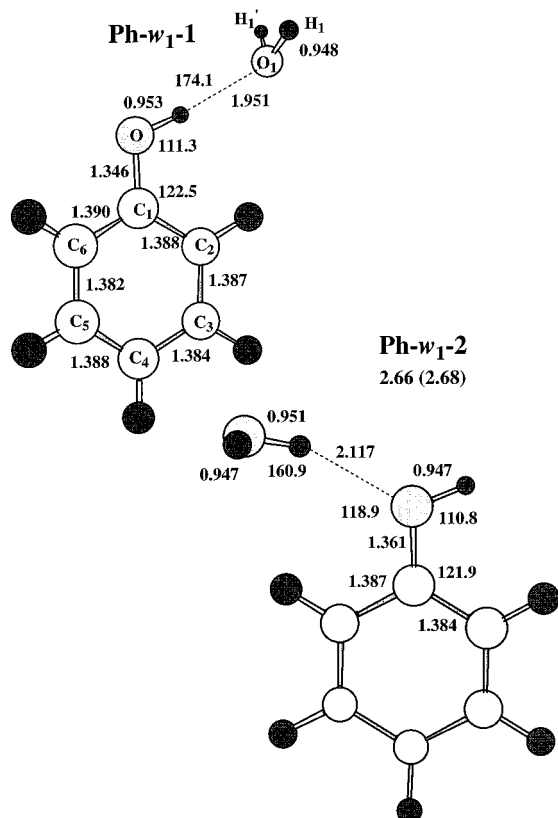


**Figure 1.** Two lower energy structures of the phenol–water<sub>1</sub> complex. The HF/A bond lengths in angstroms and bond angles in degrees are displayed. The corresponding MP2/A geometrical parameters of Ph-w<sub>1</sub>-1 are the following:  $r(\text{O}-\text{H}) = 0.983 \text{ \AA}$ ,  $r(\text{O}_1-\text{H}_1) = 1.867 \text{ \AA}$ ,  $r(\text{O}_1-\text{H}_1) = 0.971 \text{ \AA}$ ,  $r(\text{O}-\text{C}_1) = 1.368 \text{ \AA}$ ,  $r(\text{C}_1-\text{C}_2) = 1.400 \text{ \AA}$ ,  $r(\text{C}_2-\text{C}_3) = 1.396 \text{ \AA}$ ,  $r(\text{C}_3-\text{C}_4) = 1.396 \text{ \AA}$ ,  $r(\text{C}_4-\text{C}_5) = 1.398 \text{ \AA}$ ,  $r(\text{C}_5-\text{C}_6) = 1.393 \text{ \AA}$ ,  $r(\text{C}_1-\text{C}_6) = 1.400 \text{ \AA}$ ,  $\angle\text{OHO}_1 = 175.3^\circ$ ,  $\angle\text{C}_1\text{OH} = 108.8^\circ$ ,  $\angle\text{OC}_1\text{C}_2 = 122.7^\circ$ . The HF/A energy relative to the global-minimum structure Ph-w<sub>1</sub>-1 is given in kcal/mol. Its MP2(sp)/A analogue is followed in parentheses. Numbering of the carbon atoms of phenol valid throughout the present work is also shown.

for this reason, the most energetically favorable site of phenol to bind a water molecule is its OH-group acting as a hydrogen bond donor. Such a phenol donor–water acceptor structure, hereafter designated as Ph-w<sub>1</sub>-1, and shown in Figure 1, lies at the bottom of the PES of Ph(H<sub>2</sub>O)<sub>1</sub>. Its binding energy of 7.35 kcal/mol calculated at the HF/A level increases to 9.54 kcal/mol when the MP2(sp)/A calculation is carried out (see Table 2). The latter value agrees with the binding energy of 9.3 kcal/mol obtained at the MP2/D95\* level.<sup>15a</sup> Due to the donating function of the phenolic O–H group in Ph-w<sub>1</sub>-1, its bond length increases by 0.006 Å compared to that in bare phenol.

A major effect of the H-bond donor functioning of phenol in the Ph-w<sub>1</sub>-1 complex is anticipated to occur in its vibrational spectrum. It is primarily manifested in a red shift by ca. 109 cm<sup>-1</sup> >  $\Delta\nu$  of the phenolic  $\nu_{OH}$  stretching vibration comparing with that of bare phenol. Furthermore, the IR intensity of  $\nu_{OH}$  increases by a factor of 6.6. This HF/A value agrees rather satisfactorily with the experimental findings by Tanabe et al.<sup>6b</sup> who reported a red shift of 133 cm<sup>-1</sup> (see also Watanabe et al.<sup>6d</sup>). The MP2/6-31G level raised it to 186 cm<sup>-1</sup>,<sup>17a</sup> whereas the B3LYP/DZP level raised it to 244 cm<sup>-1</sup>.<sup>15c</sup> This actually shows a one side of the IR pattern. The other one originates from that such H-bond donor binding of phenol with water does not significantly affect the stretching vibrations of water:  $\nu_1$  and  $\nu_3$  are changed by only 1 and 6 cm<sup>-1</sup>, respectively. We may thus conclude that the H-bond donation of phenol to water molecule taking place in the global minimum energy Ph-w<sub>1</sub>-1 structure weakens the phenolic OH stretching vibration and breaks the order of the OH-frequencies of the isolated phenol and water deduced in eq 1 in such a way that  $\nu_{OH}$  has a lower wavenumber compared to  $\nu_1$ , viz.,

$$\begin{aligned} \text{exptl: } \nu_{OH} &< \nu_1^a < \nu_3^a \\ \text{HF/A: } \nu_{OH} &< \nu_1^a < \nu_3^a \\ \text{MP2/A: } \nu_{OH} &< \nu_1^a < \nu_3^a \end{aligned} \quad (2)$$

where the superscript “a” stands for an *acceptor* of hydrogen bonding emphasizing a role of water molecule. In the other words, this merges into a “window” region of ~113–133 cm<sup>-1</sup> width. The hydrogen bonding between phenol and water molecule also gives rise to the H-bond stretching  $\nu_\sigma$  at 158.5 (182.2) cm<sup>-1</sup> (the experimental value ranges between 151 and 163 cm<sup>-1</sup>; see Table 2 in ref 15a). Interestingly, the torsional mode  $\tau_{OH}$  of phenol is substantially blue shifted to 719.3 (775.5) cm<sup>-1</sup> (the B3LYP/D95\* value is 447 cm<sup>-1</sup> 15a).

The lowest energy local minimum on the PES of Ph(H<sub>2</sub>O)<sub>1</sub> is occupied by the Ph-w<sub>1</sub>-2 structure shown in Figure 1. Here, phenol acts as an acceptor of hydrogen bond, and compared to the hydrogen bond donor structure, it is less favorable, by 2.66 kcal/mol at the HF/A level (see also ref 17a). The energy difference between Ph-w<sub>1</sub>-1 and Ph-w<sub>1</sub>-2 slightly reduces to 2.59 kcal/mol after taking the ZPVE correction into account and increases to 2.68 kcal/mol if both structures are recalculated at the MP2(sp)/A level.

A particular disfavor of the hydrogen bond acceptor functioning of phenol in Ph-w<sub>1</sub>-2 results in that the O–H...O<sub>1</sub> bond length elongates by 0.12 Å in Ph-w<sub>1</sub>-2 compared to that in Ph-



**TABLE 2: Relative Energies, ZPVEs, Enthalpies (in kcal/mol), and Entropies (in cal/mol T) of Ph(H<sub>2</sub>O)<sub>n</sub> Complexes<sup>a</sup>**

Ph(H <sub>2</sub> O) <sub>n</sub>	$\Delta$ energy <sub>HF</sub>	$\Delta$ energy <sub>MP2(sp)</sub>	ZPVE	$\Delta$ enthalpy	$\Delta$ entropy
Ph-w <sub>1</sub> -1	7.35	9.54	0.0	0.0	0.0
Ph-w <sub>1</sub> -2	4.70	6.86	-0.03	2.59	0.78
Ph-w <sub>2</sub> -1,2	10.43	14.80	0.0	0.0	0.0
Ph-w <sub>3</sub> -1,1'	11.65	15.25	0.0	0.0	0.0
Ph-w <sub>3</sub> -2,2'	11.13	14.64	-0.15	0.45	-1.44
Ph-w <sub>3</sub> -3	10.77	14.21	-0.11	0.75	-2.86
Ph-w <sub>3</sub> -4	9.01	12.28 (2.46 <sup>a</sup> )	-0.56	2.30	-2.91
Ph-w <sub>4</sub> -1	9.57	12.36	0.0	0.0	0.0
Ph-w <sub>4</sub> -2	8.08	12.47 (-1.09 <sup>a</sup> 0.96 <sup>b</sup> -0.07 <sup>c</sup> )	-0.53 (1.07 <sup>c</sup> )	1.73	-6.38
Ph-w <sub>4</sub> -3	8.49	12.80 (-0.89 <sup>a</sup> 0.45 <sup>c</sup> )	-0.52 (1.09 <sup>c</sup> )	1.28	-7.19
Ph-w <sub>4</sub> -4	8.05	12.25 (-0.55 <sup>a</sup> 0.67 <sup>b</sup> 0.93 <sup>c</sup> )	-0.02 (0.33 <sup>c</sup> )	1.56	-3.81
Ph-w <sub>4</sub> -5	7.95	12.04	0.08	1.63	-2.96
Ph-w <sub>4</sub> -6	8.63	11.92	-0.23	1.09	-2.13
Ph-w <sub>4</sub> -7	8.26	11.92	0.10	1.26	-1.74
Ph-w <sub>4</sub> -8	8.30	11.79	-0.28	1.38	-3.05
Ph-w <sub>4</sub> -9	9.00	11.50	0.25	0.47	2.62
Ph-w <sub>4</sub> -10	6.84	9.32	0.10	2.70	2.06
Ph-w <sub>4</sub> -11	5.15	8.61	0.35	4.30	0.11

<sup>a</sup> Relative energy of Ph(H<sub>2</sub>O)<sub>n</sub> is defined as  $-[E(\text{Ph}(\text{H}_2\text{O})_n) - E(\text{Ph}) - (nE(\text{H}_2\text{O}))]$ . Table also includes the relative MP2/A<sup>a</sup>, MP2/A<sup>+b</sup>, and B3LYP/A<sup>c</sup> energies with respect to the structure 1 of the phenol-water<sub>n</sub> complex.

**TABLE 3: Theoretical Rotational Constants A, B, and C in GHz and Total Dipole Moment in D of Ph(H<sub>2</sub>O)<sub>n</sub> Complexes Calculated via the HF, MP2<sup>a</sup>, and B3LYP<sup>b</sup> Methods in Conjunction with a Basis Set**

Ph(H <sub>2</sub> O) <sub>n</sub>	A	B	C	dipole
Ph-w <sub>1</sub> -1	4.38507	1.08337	0.87222	3.92
	4.25523 <sup>a</sup>	1.11400 <sup>a</sup>	0.88657 <sup>a</sup>	3.89 <sup>a</sup>
Ph-w <sub>1</sub> -2	4.09796	1.11817	0.88142	3.56
Ph-w <sub>2</sub> -1	2.70968	0.73097	0.63654	1.15
	2.53870 <sup>a</sup>	0.83238 <sup>a</sup>	0.75134 <sup>a</sup>	1.10 <sup>a</sup>
Ph-w <sub>3</sub> -1	1.94209	0.50448	0.42647	1.16
	1.89925 <sup>a</sup>	0.54336 <sup>a</sup>	0.46239 <sup>a</sup>	1.14 <sup>a</sup>
Ph-w <sub>3</sub> -2	1.91922	0.51563	0.44259	1.13
Ph-w <sub>3</sub> -3	1.86586	0.52443	0.45787	1.52
Ph-w <sub>3</sub> -4	1.45663	0.69364	0.59343	1.98
	1.46994 <sup>a</sup>	0.78406 <sup>a</sup>	0.66417 <sup>a</sup>	1.94 <sup>a</sup>
Ph-w <sub>4</sub> -1	1.31037	0.37687	0.31183	0.96
	1.21338 <sup>a</sup>	0.44044 <sup>a</sup>	0.36928 <sup>a</sup>	1.17 <sup>a</sup>
	1.32264 <sup>b</sup>	0.41360 <sup>b</sup>	0.34133 <sup>b</sup>	1.25 <sup>b</sup>
Ph-w <sub>4</sub> -2	1.14775	0.53379	0.47190	2.58
	1.11526 <sup>a</sup>	0.70260 <sup>a</sup>	0.61283 <sup>a</sup>	2.34 <sup>a</sup>
	1.21478 <sup>b</sup>	0.57219 <sup>b</sup>	0.49779 <sup>b</sup>	2.55 <sup>b</sup>
Ph-w <sub>4</sub> -3	1.51720	0.43861	0.41398	3.55
	1.55673 <sup>a</sup>	0.49177 <sup>a</sup>	0.46151 <sup>a</sup>	3.82 <sup>a</sup>
	1.59183 <sup>b</sup>	0.46947 <sup>b</sup>	0.44238 <sup>b</sup>	3.69 <sup>b</sup>
Ph-w <sub>4</sub> -4	1.21216	0.51396	0.45024	2.48
	1.25108 <sup>a</sup>	0.56229 <sup>a</sup>	0.50145 <sup>a</sup>	2.92 <sup>a</sup>
	1.29591 <sup>b</sup>	0.54344 <sup>b</sup>	0.48837 <sup>b</sup>	2.42 <sup>b</sup>
Ph-w <sub>4</sub> -5	1.18647	0.52433	0.45296	1.73
Ph-w <sub>4</sub> -6	1.58475	0.34963	0.30846	3.23
Ph-w <sub>4</sub> -7	1.03920	0.52807	0.49064	1.11
Ph-w <sub>4</sub> -8	1.14855	0.47892	0.40965	2.35
Ph-w <sub>4</sub> -9	1.26070	0.37569	0.310086	0.92
Ph-w <sub>4</sub> -10	1.26992	0.35619	0.31544	2.37
Ph-w <sub>4</sub> -11	1.13115	0.49384	0.47181	1.56

w<sub>1</sub>-1 and appears more bent by 13.2°. It also causes the elongation of the C—O bond by ca. 0.1 Å compared to its value in bare phenol and does not practically distort the angles linked to the C—O—H bond of phenol and the  $\angle\text{H}_1\text{O}_1\text{H}'_1$  bond angle of water molecule as well. In the two above-mentioned structures, there exists a weak interaction between the oxygen atom of water molecule and the *ortho* hydrogen atom of the phenol ring that is indicated by the corresponding distances of 2.875 Å and 2.727 Å for Ph-w<sub>1</sub>-1 and Ph-w<sub>1</sub>-2, respectively. The rotational constants and the total dipole moment of both reported Ph-w<sub>1</sub> structures are gathered in Table 3. As seen there, the H-bond donor structure is more polar than the H-bond acceptor one. There is still another feature which distinguishes

the two studied structures of phenol with water molecule from each other: if in the global minimum energy one, the oxygen atom of water molecule resides in the phenol plane, in Ph-w<sub>1</sub>-2, on the contrary, it lies out-of-plane forming the dihedral angle of 95.0°. We explain this by the directionality of the lone pair of the phenolic oxygen. It implies that there are actually two isomers of Ph-w<sub>1</sub>-2: one where the oxygen atom of water molecule is placed above the phenol ring and the other one where it lies below. Such a feature remains if more water molecules interact with phenol. We consider this as one of the reasons of an appearance of  $\pi$  hydrogen bonding after adding a sufficient number of water molecules to phenol: the cyclic arrangement of water molecules becomes exhausted and the energetical favor turns to three-dimensional water patterns.

Comparing with Ph-w<sub>1</sub>-1, the symmetric  $\nu_1$  and asymmetric  $\nu_3$  vibrations in Ph-w<sub>1</sub>-2 are red shifted by 13 and 18 cm<sup>-1</sup>, while the phenol  $\nu_{\text{OH}}$  stretching vibration is downshifted by only 4 cm<sup>-1</sup>. Therefore, the stretching IR pattern of Ph-w<sub>1</sub>-2 appears to be the following:

$$\nu_1^{\text{d}} 57 < \nu_{\text{OH}} 56 < \nu_3^{\text{d}} \quad (3)$$

Notice that the IR pattern inherent for isolated phenol and water molecules (eq 1) is nearly retained in the Ph-w<sub>1</sub>-2 structure. The H-bond vibrational mode  $\nu_{\sigma} = 125.5$  cm<sup>-1</sup> is lower than that in Ph-w<sub>1</sub>-1, implying that the hydrogen bonding in the Ph-w<sub>1</sub>-1 structure is stronger.

Let us now proceed to the PES of Ph(H<sub>2</sub>O)<sub>2</sub> whose lower energy portion is displayed in Figure 2. Two ring isomers, Ph-w<sub>2</sub>-1 and Ph-w<sub>2</sub>-2 (obtained from Ph-w<sub>2</sub>-1 by applying the reflection relative to the phenol plane), reside at its global energy minimum. In these structures, the OH-group of phenol acts bilaterally, as the H-bond donor and H-bond acceptor as well. The three H-bonds in Ph-w<sub>2</sub>-1 are rather bent (see Figure 2). The hydrogen bond between the phenol H-bond acceptor and the water molecule donor ( $w_{\text{ad}1}$ ) is relatively long (2.138 Å).

Five calculated OH stretching vibrations of the Ph-w<sub>2</sub>-1 structure are gathered in Table 1. By analogy with the Ph-w<sub>1</sub>-1 complex, the hydrogen bonded phenolic  $\nu_{\text{OH}}$  vibration is red shifted by 202 cm<sup>-1</sup> and its IR intensity is enhanced by a factor of 4.9 while its Raman activity only doubles. The other four vibrations are simply assigned to the  $\nu_1$  and  $\nu_3$  of water molecules  $w_{\text{ad}1}$  and  $w_{\text{ad}2}$  although their collective nature essential

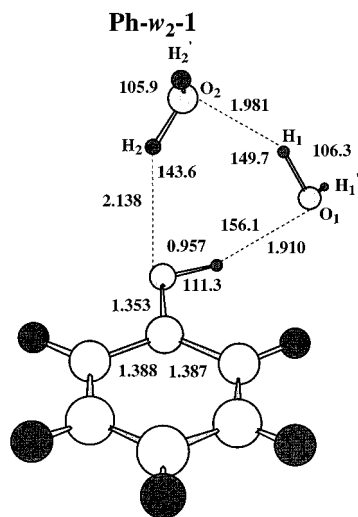


**Figure 2.** The lowest energy structure of the phenol–water<sub>2</sub> complex. The HF/A bond lengths in angstroms and bond angles in degrees are shown. The corresponding MP2/A values are the following:  $r(\text{O}-\text{H}) = 0.992 \text{ \AA}$ ,  $r(\text{O}_1-\text{H}) = 1.811 \text{ \AA}$ ,  $r(\text{O}_2-\text{H}_1) = 1.846 \text{ \AA}$ ,  $r(\text{O}-\text{H}_2) = 1.994 \text{ \AA}$ ,  $\angle\text{OHO}_1 = 155.7^\circ$ ,  $\angle\text{O}_1\text{H}_1\text{O}_2 = 151.5^\circ$ ,  $\angle\text{O}_2\text{H}_2\text{O} = 145.3^\circ$ .

for larger water clusters around phenol should be noticed. One pair of them,  $\nu_1^{\text{ad1}}$  and  $\nu_3^{\text{ad1}}$ , at 3973.2 and 4147.1  $\text{cm}^{-1}$  corresponds to symmetric and asymmetric stretchings of the water molecule  $w_{\text{ad1}}$  accepting the phenolic hydrogen bond and donating the hydrogen bond to water dimer. The other one,  $\nu_1^{\text{ad2}}$  and  $\nu_3^{\text{ad2}}$ , centered at 4021.7 and 4154.7  $\text{cm}^{-1}$ , describes the symmetric and asymmetric OH stretching vibrations of the water molecule  $w_{\text{ad2}}$  donating the hydrogen bond to phenol and accepting the other one from  $w_{\text{ad1}}$ . Altogether, they are red shifted and considerably enhanced compared with the similar vibrations in water and monohydrated phenol. Summarizing, the IR stretching region becomes patterned in this manner,

$$\begin{aligned} \text{exptl: } \nu_{\text{OH}} &< \nu_1^{\text{ad1}} < \nu_1^{\text{ad2}} < \nu_3^{\text{ad1}} < \nu_3^{\text{ad2}} \\ \text{HF/A: } \nu_{\text{OH}} &< \nu_1^{\text{ad1}} < \nu_1^{\text{ad2}} < \nu_3^{\text{ad1}} < \nu_3^{\text{ad2}} \\ \text{MP2/A: } \nu_{\text{OH}} &< \nu_1^{\text{ad1}} < \nu_1^{\text{ad2}} < \nu_3^{\text{ad1}} < \nu_3^{\text{ad2}} \end{aligned} \quad (4)$$

In eq 4, we thus observe the MP2/A “window” region of the 184  $\text{cm}^{-1}$  width. Compared to that reported above for the phenol–water<sub>1</sub> complex and demonstrated in eq 2, it is extended by 51  $\text{cm}^{-1}$ . As clearly follows from Table 1, its extension originates, first, from a further red shift by 177  $\text{cm}^{-1}$  of the phenolic OH stretching compared to Ph- $w_1$ -1 as a result of a stronger H-bonding donation of the OH-group of phenol to water dimer. Despite the fact that the corresponding  $\nu_\sigma$  frequency is less by 21  $\text{cm}^{-1}$  than that in Ph- $w_1$ -1 due to likely a more bending character of the related hydrogen bond, the H-bonding is stronger since the phenolic O–H bond pursues to elongate by 0.009  $\text{\AA}$ . Second, it also originates from a rather substantial red shift of 203  $\text{cm}^{-1}$  taking place in water dimer where the corresponding H-bridge stretching frequency reaches the value of 245.2  $\text{cm}^{-1}$ . And finally, third, it stems out from a strengthening of the H-bonding donation of water dimer to the lone pair electrons of the phenolic OH-group as particularly indicated by the  $\nu_\sigma$  frequency equal to 201.2  $\text{cm}^{-1}$  which exceeds the analogous one in Ph- $w_2$ -1 by a factor of 1.8. Notice at last that the  $\nu_1$  mode of the water molecule  $w_{\text{ad2}}$  playing role of a donor of hydrogen bond to phenol borders the left-hand

side of the “window” region. This is a typical feature for the cyclic arrangements of water molecules bonded to phenol. We will observe it for the Ph( $\text{H}_2\text{O}$ )<sub>3</sub> complex in the following Section.

**3.B. Lower Energy Structures of Ph( $\text{H}_2\text{O}$ )<sub>3</sub>.** Adding a third water molecule to the Ph( $\text{H}_2\text{O}$ )<sub>2</sub> complex significantly enriches the PES landscape of Ph( $\text{H}_2\text{O}$ )<sub>3</sub>. This is clearly seen in Figure 3 displaying four lower energy structures of phenol bonded to three water molecules. The global minimum is occupied by two isoenergetic structures, Ph- $w_3$ -1 and Ph- $w_3$ -1', converting into each other via the plane of symmetry of phenol perpendicular to the phenol ring. These structures possess a closed cyclic water pattern  $S_3$  to which the phenolic OH-group simultaneously donates and accepts hydrogen bonds. A similar water pattern is inherent for Ph- $w_3$ -2 (its isomer is Ph- $w_3$ -2') and Ph- $w_3$ -3 (isomer Ph- $w_3$ -3') lying within ca. 1 kcal/mol above the global minimum and reported in the present work for the first time. Their difference from the global minimum isomers originates from flippings of free OH groups of water molecules which can be classified by the “u” and “d” symbols (see, e.g., ref 5d). In this regard, it is worth mentioning that the structure reported in ref 17a as the most energetically close to the global minimum lies 2.57 kcal/mol above it.

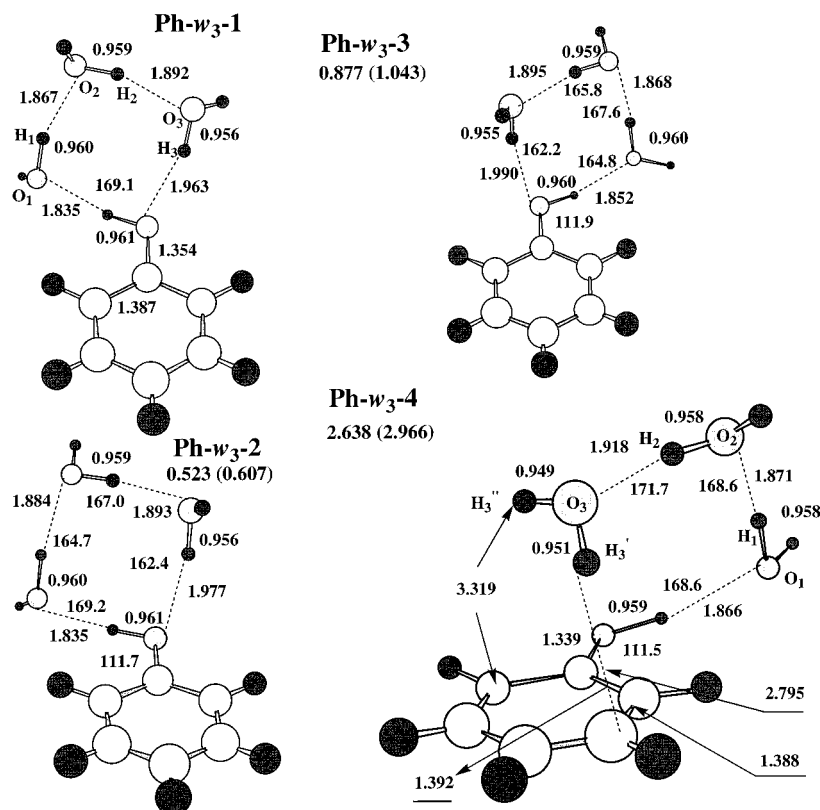
Analyzing the global minimum structures shown in Figures 1–3, we reveal a tendency of systematic shortening of the phenol–water hydrogen bonds with adding of an extra water molecule. Namely, the length of the phenol donor–water acceptor H-bond varies from 1.95  $\text{\AA}$  in Ph- $w_1$  to 1.91  $\text{\AA}$  in Ph- $w_2$  and, finally, to 1.83  $\text{\AA}$  in Ph- $w_3$ . This fairly correlates with the recent experimental findings reported in ref 10b. On the other hand, passing from Ph- $w_2$  to Ph- $w_3$ , the water donor–phenol acceptor phenol–water hydrogen bond shortens by 0.18  $\text{\AA}$ .

Table 4 collects seven theoretical OH stretching vibrations of the five lower energy Ph- $w_3$  structures relevant to discuss a “window” region. Inspecting this Table, we may notice that they are actually gathered in two rather well separated groups. Considering the Ph- $w_3$ -1 structure as an example, we find that the first group is composed of four highly IR intensive vibrations placed between 3835 and 3983  $\text{cm}^{-1}$  and describing cooperative stretching vibrations of the intraring OH-bonds. The first two of them are dominantly assigned to the coupled OH stretching vibration of phenol and its nearest-neighbor OH-bond O<sub>1</sub>–H<sub>1</sub> (see Figure 3). The lower wavenumber vibration, corresponding to the symmetric stretch of these OH-bonds, is rather Raman active and red shifted by 283  $\text{cm}^{-1}$  with respect to the OH stretching frequency of bare phenol. The other one is less red shifted, by 223  $\text{cm}^{-1}$ . The second group of vibrations is comprised of three vibrations lying between 4142 and 4148  $\text{cm}^{-1}$ . The OH stretching vibrations of three free OH-groups of water molecules dominantly contribute to this group. They are shifted to lower wavenumbers relative to the  $\nu_3$  vibration of water molecule by approximately 40  $\text{cm}^{-1}$ . The separation between these groups, which determines a width of the “window” region, amounts to 307  $\text{cm}^{-1}$  at the HF/A level and to 267  $\text{cm}^{-1}$  for the MP2/A calculation. In the other words, the stretching IR pattern of the Ph- $w_3$ -1 structure takes the following form

$$\begin{aligned} \text{MP2/A: } \nu_{\text{OH}} &< \nu_1^{\text{ad1}} < \nu_1^{\text{ad2}} < \nu_3^{\text{ad3}} \\ &< \nu_3^{\text{ad1}} < \nu_3^{\text{ad2}} < \nu_3^{\text{ad3}} \end{aligned} \quad (5)$$

where the experimental spacings<sup>6d</sup> are given in parentheses.

The fourth structure of the Ph- $w_3$  complex reported in the present work for the first time and displayed in Figure 3 is rather



**Figure 3.** Four lower energy structures of the phenol–water<sub>3</sub> complex. The HF/A bond lengths in angstroms and bond angles in degrees are indicated. The corresponding MP2/A values for Ph- $w_3$ -1 and Ph- $w_3$ -4 are the following. (i) Ph- $w_3$ -1:  $r(\text{O}-\text{H}) = 0.999 \text{ \AA}$ ,  $r(\text{O}_1-\text{H}) = 1.715 \text{ \AA}$ ,  $r(\text{O}_1-\text{H}_1) = 0.993 \text{ \AA}$ ,  $r(\text{O}_2-\text{H}_1) = 1.750 \text{ \AA}$ ,  $r(\text{O}_2-\text{H}_2) = 0.990 \text{ \AA}$ ,  $r(\text{O}_3-\text{H}_2) = 1.780 \text{ \AA}$ ,  $r(\text{O}_3-\text{H}_3) = 0.985 \text{ \AA}$ ,  $r(\text{O}-\text{H}_3) = 1.831 \text{ \AA}$ ,  $r(\text{C}_1-\text{O}) = 1.378 \text{ \AA}$ ,  $r(\text{C}_1-\text{C}_6) = 1.399 \text{ \AA}$ ,  $\angle\text{OHO}_1 = 170.1^\circ$ ,  $\angle\text{O}_1\text{H}_1\text{O}_2 = 167.6^\circ$ ,  $\angle\text{O}_2\text{H}_2\text{O}_3 = 168.2^\circ$ ,  $\angle\text{O}_3\text{H}_3\text{O} = 164.8^\circ$ ,  $\angle\text{C}_1\text{OH} = 109.4^\circ$ . (ii) Ph- $w_3$ -4:  $r(\text{O}-\text{H}) = 0.995 \text{ \AA}$ ,  $r(\text{O}_1-\text{H}) = 1.750 \text{ \AA}$ ,  $r(\text{O}_1-\text{H}_1) = 0.991 \text{ \AA}$ ,  $r(\text{O}_2-\text{H}_1) = 1.757 \text{ \AA}$ ,  $r(\text{O}_2-\text{H}_2) = 0.987 \text{ \AA}$ ,  $r(\text{O}_3-\text{H}_2) = 1.815 \text{ \AA}$ ,  $r(\text{O}_3-\text{H}_3) = 0.975 \text{ \AA}$ ,  $r(\text{O}_3-\text{H}_3') = 0.972 \text{ \AA}$ ,  $r(\text{C}_1-\text{O}) = 1.356 \text{ \AA}$ ,  $r(\text{C}_1-\text{C}_2) = 1.405 \text{ \AA}$ ,  $r(\text{C}_2-\text{C}_3) = 1.399 \text{ \AA}$ ,  $r(\text{C}_3-\text{H}_3') = 2.441 \text{ \AA}$ ,  $r(\text{C}_6-\text{H}_3') = 2.909 \text{ \AA}$ ,  $\angle\text{OHO}_1 = 167.1^\circ$ ,  $\angle\text{O}_1\text{H}_1\text{O}_2 = 173.5^\circ$ ,  $\angle\text{O}_2\text{H}_2\text{O}_3 = 175.5^\circ$ ,  $\angle\text{C}_1\text{OH} = 108.8^\circ$ . The HF/A (MP2(sp)/A) relative energy with respect to the global-minimum structure Ph- $w_3$ -1 is given in kcal/mol.

peculiar in the following sense. As shown in Figure 3, one of its terminal water molecules accepts the phenolic OH-group. The other one,  $\text{O}_3\text{H}_3'\text{H}_3''$ , lies above the phenol ring. It forms a so-called  $\pi$  hydrogen bond with the  $\pi$  cloud of this ring, partly similar to the Leg2-type benzene–water structure discussed in ref 20b. The shortest MP2/A distance of  $2.441 \text{ \AA}$  is predicted between the  $\text{H}_3''$  and the carbon atom  $\text{C}_3$  (see Figure 3). The other one  $r(\text{H}_3'-\text{C}_6) = 2.909 \text{ \AA}$  almost coincides with the sum of van der Waals radii of the corresponding atoms. Compared to free water molecule, both O–H bond lengths undergo tiny elongations, about  $0.003\text{--}0.006 \text{ \AA}$ . However, contrary to the other water molecules belonging to this structure as well as to all water molecules in the aforementioned structures of phenol–water where the hydrogen bonding causes an increase of the HOH bond angle, the water molecule participating in the  $\pi$  hydrogen bonding with phenol ring shows an opposite effect: its bond angle  $\angle\text{HOH}$  decreases by  $1.3^\circ$ . This is, in turn, manifested in the bending vibrations of water molecules. If two of them,  $w_1$  and  $w_2$ , are characterized by the bending frequencies  $\nu_2$  centered at  $1762$  and  $1788 \text{ cm}^{-1}$  which are red shifted by  $27$  and  $52 \text{ cm}^{-1}$  compared to the bending frequency in water monomer, the third water molecule  $w_3$  possesses the scissor frequency of  $1742 \text{ cm}^{-1}$  resulting in a blue shift of  $7 \text{ cm}^{-1}$ .

The novel Ph- $w_3$ -4 structure has the largest total dipole moment of  $1.98 \text{ D}$  among all reported lower energy Ph- $w_3$  structures. This is shown in Table 3. It is also more compact as follows from the comparison of the rotational constants of all Ph- $w_3$  structures given in Table 3. Energetically, Ph- $w_3$ -4 resides  $2.64 \text{ kcal/mol}$  (HF/A) and  $2.46 \text{ kcal/mol}$  (MP2/A) above the

global minimum structure Ph- $w_3$ -1. These values decrease to  $2.08$  and  $1.83 \text{ kcal/mol}$ , correspondingly, after taking the ZPVE corrections into account. Comparing free energies of the lower lying Ph- $w_3$  structures determined by their enthalpies and entropies listed in Table 2, we conclude that, at  $T \geq 262.8 \text{ K}$ , Ph- $w_3$ -3 becomes the most energetically favorable structure. In terms of free energy, it also lies below Ph- $w_3$ -2 at  $T \geq 209.7 \text{ K}$ . The latter appears more favorable at  $T \geq 315.3 \text{ K}$  than Ph- $w_3$ -1. At room temperature,  $T = 298.15 \text{ K}$ , the free energy of Ph- $w_3$ -4 is greater than that of Ph- $w_3$ -2 by only  $1.54 \text{ kcal/mol}$ .

Regarding the novel Ph- $w_3$ -4 structure, its seven OH stretching vibrations are nonseparable into two distinct groups. It is also worth mentioning that, in contrast to the IR stretching pattern of Ph- $w_3$ -1 which spans over the region of  $580$  wavenumbers, the IR stretching pattern of the Ph- $w_3$ -4 is narrower, about  $500$  wavenumbers. Its most red-shifted vibration predicted at  $3870$  ( $3352$ )  $\text{cm}^{-1}$  is mainly attributed to the collective stretching vibration of the phenolic OH-group and the OH-group of the water molecule which plays a role of the H-bond acceptor of phenol (see Table 4). Such feature looks drastically different from what we have already observed for the Ph- $w_3$ -1 complex whose most red-shifted stretching vibration is substantially localized on the OH-group of phenol. The second vibration of Ph- $w_3$ -4 placed at  $\approx 3920$  ( $3467$ )  $\text{cm}^{-1}$  is characterized by the highest IR absorption equal to  $773$  ( $994$ )  $\text{km/mol}$  among all reported Ph- $w_3$  structures. Together with the third vibration at  $3951$  ( $3549$ )  $\text{cm}^{-1}$ , these vibrations describe the coupled stretchings of phenolic and water OH-bonds. The fourth vibrational mode with the frequency of  $4055$  ( $3733$ )  $\text{cm}^{-1}$  is

**TABLE 4: The OH Stretch Frequencies, in cm<sup>-1</sup>, of Phenol–Water<sub>3</sub> Complexes Calculated at the HF/A and MP2/A (in Parentheses) Computational Levels<sup>a</sup>**

frequency	IR	Raman	assignment
Ph-w <sub>3</sub> -1,1'			
3834.7 (3273.4)	537 (821)	213	$\nu_{\text{OH}}, \nu_{\text{O}_1\text{H}_1}$ (33.8%)
3895.4 (3418.8)	602 (755)	50	$\nu_{\text{O}_1\text{H}_1}, \nu_{\text{OH}}$ (69.9%), $\nu_{\text{O}_2\text{H}_2}$ (56.3%)
3929.3 (3496.1)	571 (973)	43	$\nu_{\text{O}_2\text{H}_2}, \nu_{\text{O}_1\text{H}_1}$ (52.7%), $\nu_{\text{O}_3\text{H}_3}$ (10.1%)
3982.8 (3578.9)	418 (616)	114	$\nu_{\text{O}_3\text{H}_3}$
4142.2 (3845.4)	136 (85)	64	$\nu_{\text{O}_1\text{H}_1'}, \nu_{\text{O}_2\text{H}_2}'$ (11.9%)
4143.8 (3850.8)	81 (80)	65	$\nu_{\text{O}_2\text{H}_2}', \nu_{\text{O}_1\text{H}_1}'$ (12.8%)
4148.3 (3853.3)	171 (107)	53	$\nu_{\text{O}_3\text{H}_3}'$
Ph-w <sub>3</sub> -2,2'			
3840.2	531	219	$\nu_{\text{OH}}, \nu_{\text{O}_1\text{H}_1}$ (24.5%), $\nu_{\text{O}_2\text{H}_2}$ (6.4%)
3901.4	629	49	$\nu_{\text{O}_1\text{H}_1}, \nu_{\text{O}_2\text{H}_2}$ (93.1%), $\nu_{\text{OH}}$ (66.5%)
3931.0	553	38	$\nu_{\text{O}_2\text{H}_2}, \nu_{\text{O}_1\text{H}_1}$ (82.7%)
3983.5	362	82	$\nu_{\text{O}_3\text{H}_3}$
4144.3	99	55	$\nu_{\text{O}_3\text{H}_3}'$
4145.2	110	47	$\nu_{\text{O}_1\text{H}_1'}, \nu_{\text{O}_2\text{H}_2}'$ (57.9%)
4146.2	129	88	$\nu_{\text{O}_2\text{H}_2}', \nu_{\text{O}_1\text{H}_1}'$ (60.3%)
Ph-w <sub>3</sub> -3			
3854.9	382	215	$\nu_{\text{OH}}, \nu_{\text{O}_1\text{H}_1}$ (67.2%), $\nu_{\text{O}_2\text{H}_2}$ (19.4%)
3903.9	739	30	$\nu_{\text{OH}}, \nu_{\text{O}_1\text{H}_1}$ (63.4%), $\nu_{\text{O}_2\text{H}_2}$ (46.2%)
3932.0	533	48	$\nu_{\text{O}_2\text{H}_2}, \nu_{\text{O}_1\text{H}_1}$ (55.9%)
3988.9	333	66	$\nu_{\text{O}_3\text{H}_3}$
4141.5	115	66	$\nu_{\text{O}_2\text{H}_2}'$
4145.8	112	44	$\nu_{\text{O}_3\text{H}_3}'$
4152.5	107	52	$\nu_{\text{O}_1\text{H}_1}'$
Ph-w <sub>3</sub> -4			
3870.2 (3351.5)	459 (683)	188	$\nu_{\text{OH}}, \nu_{\text{O}_1\text{H}_1}$ (74.1%)
3919.8 (3467.4)	773 (994)	33	$\nu_{\text{OH}}, \nu_{\text{O}_1\text{H}_1}$ (80.3%), $\nu_{\text{O}_2\text{H}_2}$ (31.2%)
3950.9 (3549.4)	305 (462)	58	$\nu_{\text{O}_2\text{H}_2}, \nu_{\text{O}_1\text{H}_1}$ (25.7%)
4054.8 (3732.9)	91 (104)	56	$\nu_{\text{O}_3\text{H}_3}, \nu_{\text{O}_3\text{H}_3}''$ (56.0%)
4142.2 (3841.9)	108 (72)	94	$\nu_{\text{O}_1\text{H}_1}'$
4147.9 (3858.4)	115 (76)	57	$\nu_{\text{O}_2\text{H}_2}$
4156.6 (3852.0)	99 (73)	34	$\nu_{\text{O}_1\text{H}_1}'', \nu_{\text{O}_3\text{H}_3}'$ (55.3%)

<sup>a</sup> Infrared intensity in km/mol, Raman (R) activity in Å<sup>4</sup>/amu. The partial contributions are evaluated as the ratio of the total displacements. The contribution of the first reported mode is referred to 100%.

assigned to the symmetric  $\pi$ -OH stretching of the  $\pi$ H-bonded O<sub>3</sub>H<sub>3</sub>' and O<sub>3</sub>H<sub>3</sub>''-groups, whereas the corresponding  $\pi$ -OH asymmetric stretch is centered at 4157 (3852) cm<sup>-1</sup>. Their MP2/A red shifts are rather small (41 and 63 cm<sup>-1</sup> compared to free water molecule), which is a typical feature of weak hydrogen bonds. The other vibrations of Ph-w<sub>3</sub>-4 found at 4142 (3842) and 4147 (3858) cm<sup>-1</sup> describe, as usual, the stretching vibrations of free OH-groups of water molecules. Altogether, these seven OH stretching vibrations give rise to the following IR pattern:

MP2/A:

$$\nu_{\text{OH}} < \nu_1^{\text{ad1}} < \nu_1^{\text{ad2}} < \nu_1^{\text{ad3}} < \nu_{\text{sym}}^{\pi} < \nu_3^{\text{ad1}} < \nu_3^{\text{ad2}} < \nu_{\text{asym}}^{\pi} < \nu_3^{\text{ad2}} \quad (6)$$

Inspecting eqs 5 and 6, we notice a narrowing of the “window” region for the  $\pi$  hydrogen-bonded structure Ph-w<sub>3</sub>-4 compared to the conventional one with the S<sub>3</sub> arrangement of water molecules. This implies that some modes of the former structure might fall in the “window” region of the latter. In the present case, these are two modes: one corresponds to  $\nu_{\text{sym}}^{\pi}$ , the other one to  $\nu_3^{\text{ad1}}$ .

Concluding this section, we would like first of all to emphasize a rather peculiar difference between the  $\nu_{\sigma}$  mode describing the conventional hydrogen bond bridge and that of the  $\pi$  hydrogen bond one. For example, in the global minimum structure, the former ones are placed at 81, 183, 226, and 265 cm<sup>-1</sup>. If the Ph-w<sub>3</sub>-4 structure is considered, there are three  $\nu_{\sigma}$  modes at 208, 246, and 300 cm<sup>-1</sup> which describe the collective stretching vibrations in the H-bond bridges O–H $\cdots$ O<sub>1</sub>, O<sub>1</sub>–H<sub>1</sub> $\cdots$ O<sub>2</sub>, and O<sub>2</sub>–H<sub>2</sub> $\cdots$ O<sub>3</sub>. The  $\nu_{\sigma}$  of the  $\pi$  bridge is centered at 140 cm<sup>-1</sup>. Interestingly, it lies between the  $\nu_{\sigma}$  of Ph-w<sub>1</sub>-1 and

that of Ph-w<sub>1</sub>-2, thus implying that the  $\pi$  hydrogen bond in Ph-w<sub>3</sub>-4 is slightly stronger compared to the conventional hydrogen bond in Ph-w<sub>1</sub>-2 where the phenolic OH-group plays a role of the hydrogen bond acceptor. After all, just readily juxtaposing the lower energy portions of the PESs of the Ph(H<sub>2</sub>O)<sub>1≤n≤4</sub> complexes, we firmly conclude that all their global minimum energy structures involve water molecule(s) arranged in a ring manner. Nevertheless, it seems that such structure for Ph(H<sub>2</sub>O)<sub>3</sub> becomes somewhat exhausted. We think that a primary reason is that at  $n \geq 3$  the hydrogen-bond acceptor ability of the phenolic OH-group becomes competitive with the  $\pi$  one. This is transparently seen in the next section for  $n = 4$  which, in a certain sense, can be treated as a border between the global minimum energy structures where water molecules are arranged into a ring ( $n \leq 3$ ) and those where water molecules accommodate a three-dimensional pattern with  $\pi$  hydrogen bonding ( $n \geq 5$ ).<sup>5b,5d</sup>

**3.C. At Bottom of PES of Ph(H<sub>2</sub>O)<sub>4</sub>.** Scrutinizing the PES of interaction of phenol with four water molecules, one finds 11 lower energy structures lying within the interval less than 3.75 kcal/mol (MP2(sp)/A) above the global minimum. These are portrayed in Figure 4. The landscape of the lower energy portion of the PES of Ph(H<sub>2</sub>O)<sub>4</sub> is the following.

Viewing its HF/A image, we find that the global minimum is occupied by the Ph-w<sub>4</sub>-1 structure with water molecules forming a ring S<sub>4</sub> via five typical hydrogen bonds. This is in fact a conventional structure already reported in the literature.<sup>17</sup> It is characterized by rather small total dipole moment of 0.96 D. Moving upward on this PES, we arrive at two energetically closer structures, Ph-w<sub>4</sub>-3 and Ph-w<sub>4</sub>-2, which are placed above the global minimum one by 1.086 and 1.494 kcal/mol, respec-



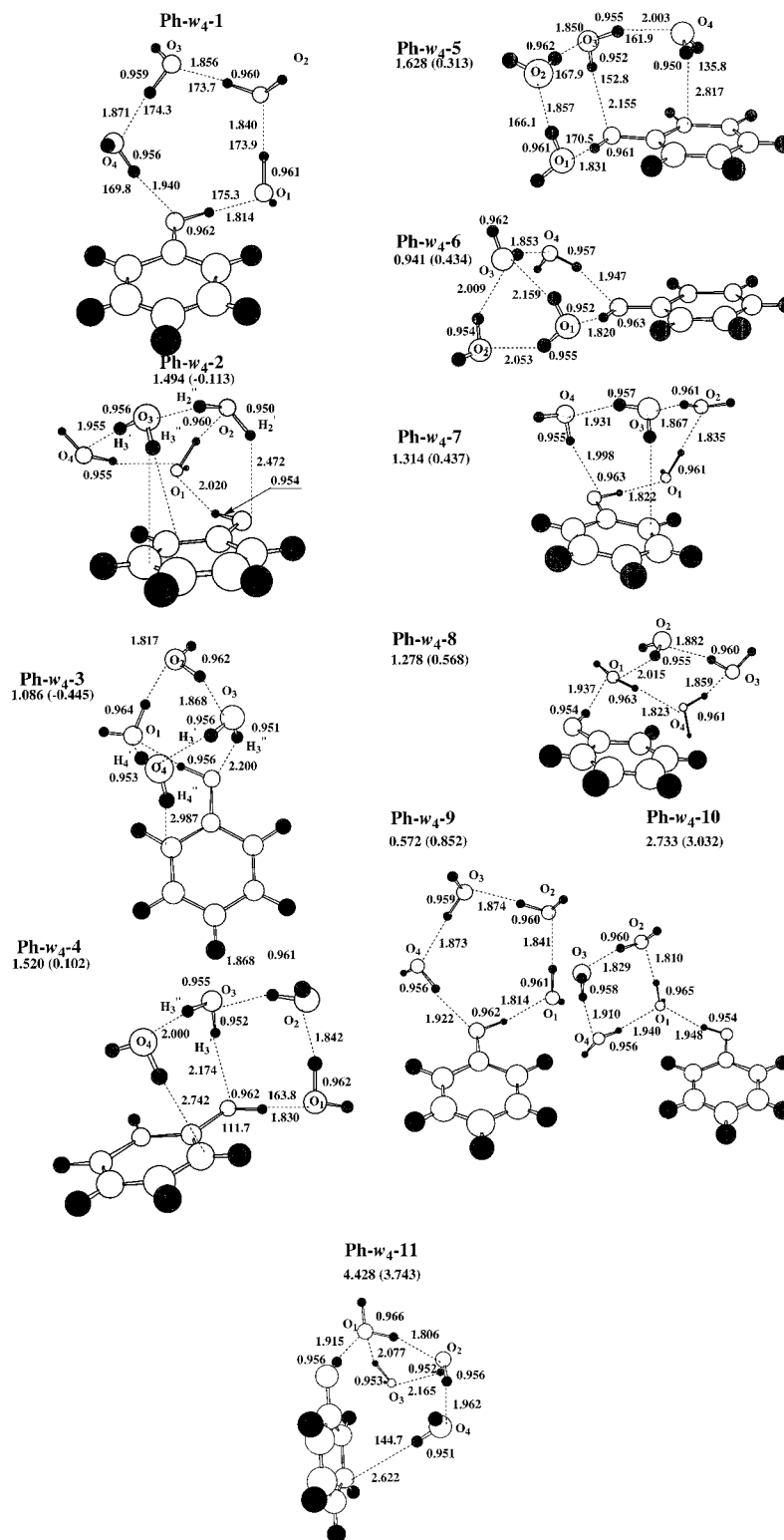


**Figure 4.** Eleven lower energy structures of the phenol–water<sub>4</sub> complex. The HF/A bond lengths in angstroms and bond angles in degrees are indicated. The corresponding MP2/A and B3LYP/A (in parentheses) values for the Ph-w<sub>4</sub>-1–4 structures are listed below. (i) Ph-w<sub>4</sub>-1:  $r(\text{O}-\text{H}) = 1.001$  (1.004) Å,  $r(\text{O}_1-\text{H}) = 1.692$  (1.646) Å,  $r(\text{O}_1-\text{H}_1) = 0.995$  (1.001) Å,  $r(\text{O}_2-\text{H}_1) = 1.723$  (1.673) Å,  $r(\text{O}_2-\text{H}_2) = 0.992$  (0.998) Å,  $r(\text{O}_3-\text{H}_2) = 1.745$  (1.695) Å,  $r(\text{O}_3-\text{H}_3) = 0.990$  (0.995) Å,  $r(\text{O}_4-\text{H}_3) = 1.767$  (1.715) Å,  $r(\text{O}_4-\text{H}_4) = 0.984$  (0.988) Å,  $r(\text{O}-\text{H}_4) = 1.828$  (1.775) Å,  $\angle\text{OHO}_1 = 175.9^\circ$  (176.9°),  $\angle\text{O}_1\text{H}_1\text{O}_2 = 176.6^\circ$  (176.3°),  $\angle\text{O}_2\text{H}_2\text{O}_3 = 175.8^\circ$  (176.9°),  $\angle\text{O}_3\text{H}_3\text{O}_4 = 174.7^\circ$  (176.7°),  $\angle\text{O}_4\text{H}_4\text{O} = 166.5^\circ$  (171.4°). (ii) Ph-w<sub>4</sub>-2:  $r(\text{O}-\text{H}) = 0.986$  (0.985) Å,  $r(\text{O}_1-\text{H}) = 1.912$  (1.852) Å,  $r(\text{O}_2-\text{H}'_2) = 0.974$  (0.974) Å,  $r(\text{O}_2-\text{H}'_2) = 0.993$  (0.998) Å,  $r(\text{O}-\text{H}'_2) = 2.221$  (2.250) Å,  $r(\text{O}_3-\text{H}'_3) = 0.972$  (0.989) Å,  $r(\text{O}_4-\text{H}'_3) = 1.860$  (1.795) Å,  $r(\text{O}_4-\text{H}_4) = 0.982$  (0.986) Å. (iii) Ph-w<sub>4</sub>-3:  $r(\text{O}-\text{H}) = 0.990$  (0.990) Å,  $r(\text{O}_1-\text{H}_1) = 1.002$  (1.010) Å,  $r(\text{O}_2-\text{H}_1) = 1.688$  (1.632) Å,  $r(\text{O}_2-\text{H}_2) = 0.997$  (1.004) Å,  $r(\text{O}_3-\text{H}_2) = 1.742$  (1.688) Å,  $r(\text{O}_3-\text{H}'_3) = 0.985$  (0.988) Å,  $r(\text{O}_3-\text{H}'_3) = 0.977$  (0.977) Å,  $r(\text{O}-\text{H}'_3) = 2.024$  (2.030) Å,  $r(\text{O}_4-\text{H}'_4) = 0.978$  (0.980) Å,  $r(\text{C}_6-\text{H}'_4) = 2.577$  (2.661) Å. (iv) Ph-w<sub>4</sub>-4:  $r(\text{O}-\text{H}) = 1.001$  (1.004) Å,  $r(\text{O}_1-\text{H}) = 1.702$  (1.747) Å,  $r(\text{O}_1-\text{H}_1) = 0.997$  (1.002) Å,  $r(\text{O}_2-\text{H}_1) = 1.719$  (1.755) Å,  $r(\text{O}_2-\text{H}_2) = 0.995$  (1.001) Å,  $r(\text{O}_3-\text{H}_2) = 1.747$  (1.771) Å,  $r(\text{O}_3-\text{H}'_3) = 0.977$  (0.978) Å,  $r(\text{O}_3-\text{H}'_3) = 0.983$  (0.985) Å,  $r(\text{O}-\text{H}'_3) = 2.000$  (2.022) Å,  $r(\text{O}_4-\text{H}'_4) = 1.885$  (1.878) Å,  $r(\text{C}_2-\text{H}_4) = 2.467$  (2.466) Å,  $\angle\text{OHO}_1 = 170.8^\circ$  (171.7°),  $\angle\text{C}_1\text{OH} = 109.3^\circ$  (110.4°). The HF/A relative energy with respect to the global-minimum structure Ph-w<sub>4</sub>-1 is given in kcal/mol. Its MP2(sp)/A analogue is followed in parentheses.



tively, after ZPVE correction. In the former one, water molecules are arranged in a sort of cage-like pattern (cf. ref 11) having six typical hydrogen bonds O–H···O and the additional O–H··· $\pi$  directed downward to the phenol ring which shows a formation of the Leg1-type  $\pi$  hydrogen bond with its  $\pi$  electrons (cf. ref 20). In the latter, water molecules form a S<sub>4</sub>-like pattern with seven hydrogen bonds distinguished, first, by the second water molecule participates in three hydrogen bonds and, second, by the third one also taking part in  $\pi$  hydrogen bonding. One of the most interesting features of these structures is an appearance of double-donor water molecules. To be more specific, this is the second water molecule in Ph-*w*<sub>4</sub>-2 and the third one in Ph-*w*<sub>4</sub>-3. Furthermore, the Ph-*w*<sub>4</sub>-3 structure has a rather peculiar pair of nonbonded oxygen atoms of water molecules, O<sub>1</sub> and O<sub>3</sub>, separated from each other by 3.426 Å which is smaller by about 0.2 Å than the first minimum of the radial oxygen–oxygen distribution function  $g_{oo}$  of liquid water widely used to define its first coordination shell (see, e.g., ref 11d and references therein).

The next, less energetically stable structures are Ph-*w*<sub>4</sub>-4 and Ph-*w*<sub>4</sub>-5. They are quite remarkably different from those considered above. Their three water molecules are arranged in the cyclic structure whereas the fourth one forms two  $\pi$  H-bonds of Leg1-type with the  $\pi$  electrons of the phenol ring. This water molecule resides above the phenol ring with distances  $r(O_4 - C_2) = 3.35$  Å and  $r(O_4 - C_3) = 3.32$  Å. The energy separations of Ph-*w*<sub>4</sub>-4 and Ph-*w*<sub>4</sub>-5 from the global minimum are 1.520 and 1.628 kcal/mol, respectively. The remainder of the lower energy portion of the PES of the Ph-*w*<sub>4</sub> complex is the following. The Ph-*w*<sub>4</sub>-6 structure has six hydrogen bonds and the total dipole moment of 3.23 D, and it is placed above the global minimum by 0.94 kcal/mol. Its water pattern also partly resembles a book. A similar structure also applies for Ph-*w*<sub>4</sub>-7, which resides above Ph-*w*<sub>4</sub>-6 by 0.37 kcal/mol. The next structure, Ph-*w*<sub>4</sub>-8, is quite particular in that its OH phenolic group functions only as a H-bond donor, in contrast to all other reported Ph-*w*<sub>4</sub> structures. The Ph-*w*<sub>4</sub>-9 structure is separated from the global minimum one by 0.572 kcal/mol. Its four water molecules form a ring similar to the Ph-*w*<sub>4</sub>-1 structure and differs from the latter by flippings of free OH-groups of water molecules. A similar water pattern is seen for Ph-*w*<sub>4</sub>-10, whereas Ph-*w*<sub>4</sub>-11 is partly similar to the Ph-*w*<sub>4</sub>-3 structure.

The MP2 and B3LYP/A PESs of Ph(H<sub>2</sub>O)<sub>4</sub> have somewhat different landscapes compared to the HF/A one due to the fact that electron correlation plays an important role in the weak interaction between phenol and water molecules. This is reflected particularly in the energetical order of the phenol–water<sub>4</sub> complexes. For example, the MP2/A method reverses this order between the Ph-*w*<sub>4</sub>-1–3 structures in such a way that Ph-*w*<sub>4</sub>-2 attains the global minimum, Ph-*w*<sub>4</sub>-3 distances from Ph-*w*<sub>4</sub>-2 by only 0.2 kcal/mol, and Ph-*w*<sub>4</sub>-1 lies above Ph-*w*<sub>4</sub>-2 by 1.1 kcal/mol (without ZPVE). It also places Ph-*w*<sub>4</sub>-4 above the global minimum by 0.54 kcal/mol. On the other hand, the B3LYP/A one locates the Ph-*w*<sub>4</sub>-3 structure at the bottom of the PES (without ZPVE correction). It is followed by Ph-*w*<sub>4</sub>-2 lying 0.38 kcal/mol above without ZPVE and 0.36 kcal/mol after ZPVE. The next structure is Ph-*w*<sub>4</sub>-1 which distances from Ph-*w*<sub>4</sub>-2 by 0.07 kcal/mol. The ZPVE corrections become quite important and reverse such order so that Ph-*w*<sub>4</sub>-1 lies beneath Ph-*w*<sub>4</sub>-2 by 0.93 kcal/mol. Ph-*w*<sub>4</sub>-4 appears then to be above Ph-*w*<sub>4</sub>-1 by 1.26 kcal/mol (after ZPVE). Summarizing and taking into account that the expected margin of error of the computational methods employed in the present work is ca.  $\pm 2$  kcal/mol, we conclude that these four structures Ph-*w*<sub>4</sub>-1–4 are

placed at the very bottom of the PES of Ph(H<sub>2</sub>O)<sub>4</sub> and are actually nearly isoenergetic. However, as follows from Table 2 and Figure 4, the MP2(sp)/A energies of the next five structures Ph-*w*<sub>4</sub>-5–9 are also close to these of Ph-*w*<sub>4</sub>-1–4, and therefore, they lie in the neighborhood of the bottom of this PES. Since the aim of the present work consists of interpreting of two distinct infrared patterns in the IR spectra of phenol–water<sub>4</sub> and because the spectroscopic patterns of these five structures Ph-*w*<sub>4</sub>-5–9 are similar to the first four (namely, Ph-*w*<sub>4</sub>-5 to Ph-*w*<sub>4</sub>-4, Ph-*w*<sub>4</sub>-6 to Ph-*w*<sub>4</sub>-3, Ph-*w*<sub>4</sub>-7, and Ph-*w*<sub>4</sub>-8 to Ph-*w*<sub>4</sub>-2, and Ph-*w*<sub>4</sub>-9 to Ph-*w*<sub>4</sub>-1, as follows after inspecting Table 5), we confine the present analysis of the IR patterns only to the latter fours.

The effect of electron correlation on the structural parameters of phenol–water<sub>4</sub> structures is also quite substantial: the equilibrium O–H bond lengths are compressed by  $\approx 0.03$ – $0.04$  Å and the O···H ones by about 0.1 Å. Notice that the difference between the MP2/A and B3LYP/A values falls within 0.003–0.005 Å for the O–H bond lengths and within 0.04–0.05 Å for the O···H distances. The O–H···O bond angles are nearly the same for all three methods. Concluding this paragraph, it is worth mentioning the geometrical parameters related to the  $\pi$  hydrogen bonds formed in the Ph-*w*<sub>4</sub>-2–4 structures. For instance, in Ph-*w*<sub>4</sub>-3, the oxygen atom O<sub>4</sub> is separated from the carbon atom C<sub>2</sub> of phenol by 3.410 Å, whereas  $r(H'_4 - C_2) = 2.661$  Å. In Ph-*w*<sub>4</sub>-2, the corresponding distances are the following:  $r(O_4 - C_3) = 3.345$  Å and  $r(H'_4 - C_2) = 2.627$  Å. The latter is smaller by about 0.3 Å than the sum of van der Waals radii of the corresponding atoms.

Let us now consider theoretical OH stretching modes of the Ph-*w*<sub>4</sub>-1–4 structures. Contrary to the Ph-*w*<sub>1</sub>-1 and Ph-*w*<sub>2</sub>-1 structures studied above, the vibrational assignments are particular for each structure of the Ph-*w*<sub>4</sub> complex. The most red-shifted OH stretching vibration at 3772 (2970.1) cm<sup>-1</sup> is predicted for the Ph-*w*<sub>4</sub>-2 structure (the corresponding B3LYP/A value is given in parentheses). It is dominantly assigned to the H stretching vibration of the O<sub>1</sub>-H<sub>1</sub>···O<sub>2</sub> bond and is significantly enhanced by a factor of 24 in comparison with the IR intensity of the  $\nu_1$  vibration of water molecule. The analogous OH stretching vibration of Ph-*w*<sub>4</sub>-3 is placed at 3798 (3008.4) cm<sup>-1</sup>. It is also dominantly assigned to the symmetric H stretching vibration of the O<sub>1</sub>-H<sub>1</sub>···O<sub>2</sub> and O<sub>2</sub>-H<sub>2</sub>···O<sub>3</sub> bonds. The corresponding asymmetric vibrational mode is found at 3874 (3201.8) cm<sup>-1</sup>. Its IR intensity exceeds that of the  $\nu_3$  vibrations of water molecule by a factor of 12. Interestingly, the phenolic OH stretching vibration contributes only to the fourth, 3988 (3476.8) cm<sup>-1</sup> and to the third, 3958 (3394.4) cm<sup>-1</sup> vibrations of Ph-*w*<sub>4</sub>-2 and Ph-*w*<sub>4</sub>-3, respectively. It is therefore red shifted by ca. 230 and 160 cm<sup>-1</sup>, respectively, from that of bare phenol and their IR intensities are increased by about 4 times. As follows from Table 5, the quintessential feature of OH stretching vibrations of the Ph-*w*<sub>4</sub>-3 and Ph-*w*<sub>4</sub>-2 is that they are nonseparable into groups of vibrations. For example, in the case of Ph-*w*<sub>4</sub>-3, the intervibration separations take the following values: 75 (192), 84 (192), 26 (67), 41 (133), 71 (76), 41 (101), 6 (11), and 4 (7) cm<sup>-1</sup> (a comparison of these values shows a significant role of correlation effects inherent for the B3LYP density functional for an adequate description of vibrational modes). We suggest that such vibrational nonseparability occurs due to the cage-type arrangements of water molecules and the existence of  $\pi$  H-bonding between one of the water molecules and the phenol ring. Such  $\pi$  H-bonding results in the corresponding  $\pi$ -OH stretching vibrations of this particular water molecule for the Ph-*w*<sub>4</sub>-3 structure being at 4024.8 (3593.9)

**TABLE 5: The OH Stretch Frequencies, in  $\text{cm}^{-1}$ , of Phenol–Water<sub>4</sub> Complexes Calculated at the HF/A and B3LYP/A (in Parentheses) Computational Levels<sup>a</sup>**

frequency	IR	Raman	assignment
Ph-w <sub>4</sub> -1			
3811.6 (3077.8)	724 (1260)	261	$\nu_{\text{OH}}$ , $\nu_{\text{O}_1\text{H}_1}$ (31.4%)
3869.0 (3217.1)	849 (1442)	68	$\nu_{\text{O}_2\text{H}_2}$ , $\nu_{\text{OH}}$ (81.1%), $\nu_{\text{O}_1\text{H}_1}$ (60.6%), $\nu_{\text{O}_3\text{H}_3}$ (32.5%)
3898.5 (3287.7)	854 (1521)	39	$\nu_{\text{O}_1\text{H}_1}$ , $\nu_{\text{O}_3\text{H}_3}$ (78.0%), $\nu_{\text{O}_2\text{H}_2}$ (21.8%)
3926.8 (3354.0)	330 (683)	73	$\nu_{\text{O}_1\text{H}_1}$ , $\nu_{\text{O}_3\text{H}_3}$ (87.6%), $\nu_{\text{O}_2\text{H}_2}$ (16.1%)
3976.6 (3468.8)	314 (551)	77	$\nu_{\text{O}_4\text{H}_4}$
4140.7 (3796.0)	112 (42)	67	$\nu_{\text{O}_1\text{H}_1'}$
4143.4 (3797.5)	105 (46)	56	$\nu_{\text{O}_2\text{H}_2}$ , $\nu_{\text{O}_3\text{H}_3'}$ (19.1%)
4143.8 (3798.7)	114 (40)	39	$\nu_{\text{O}_4\text{H}_4'}$
4144.8 (3800.3)	92 (44)	70	$\nu_{\text{O}_3\text{H}_3'}$ , $\nu_{\text{O}_2\text{H}_2'}$ (16.3%)
Ph-w <sub>4</sub> -2			
3771.8 (2970.1)	431 (772)	91	$\nu_{\text{O}_1\text{H}_1}$
3915.1 (3299.0)	309 (544)	52	$\nu_{\text{O}_2\text{H}_2}$
3961.7 (3429.8)	277 (315)	37	$\nu_{\text{O}_3\text{H}_3}$ , $\nu_{\text{O}_4\text{H}_4}$ (90.4%)
3987.7 (3476.8)	308 (987)	55	$\nu_{\text{O}_3\text{H}_3}$ , $\nu_{\text{O}_4\text{H}_4}$ (88.7%), $\nu_{\text{OH}}$ (22.7%)
4005.6 (3515.8)	416 (373)	110	$\nu_{\text{OH}}$ , $\nu_{\text{O}_4\text{H}_4}$ (18.2%)
4109.6 (3721.9)	130 (80)	33	$\nu_{\text{O}_2\text{H}_2'}$
4132.7 (3763.5)	164 (115)	47	$\nu_{\text{O}_3\text{H}_3'}$
4133.6 (3794.8)	96 (51)	95	$\nu_{\text{O}_1\text{H}_1'}$
4151.9 (3802.8)	126 (51)	80	$\nu_{\text{O}_4\text{H}_4'}$
Ph-w <sub>4</sub> -3			
3798.4 (3008.4)	448 (77)	153	$\nu_{\text{O}_1\text{H}_1}$ , $\nu_{\text{O}_2\text{H}_2}$ (22.9%)
3873.6 (3201.8)	719 (1309)	36	$\nu_{\text{O}_2\text{H}_2}$ , $\nu_{\text{O}_1\text{H}_1}$ (23.8%)
3957.6 (3394.4)	361 (572)	73	$\nu_{\text{OH}}$
3983.7 (3461.4)	244 (402)	54	$\nu_{\text{O}_3\text{H}_3'}$ , $\nu_{\text{O}_3\text{H}_3''}$ (16.8%)
4024.8 (3593.9)	163 (300)	54	$\nu_{\text{O}_4\text{H}_4'}$ , $\nu_{\text{O}_4\text{H}_4''}$ (30.5%)
4095.7 (3670.3)	218 (247)	56	$\nu_{\text{O}_3\text{H}_3'}$ , $\nu_{\text{O}_3\text{H}_3''}$ (17.9%)
4136.5 (3792.2)	111 (38)	77	$\nu_{\text{O}_1\text{H}_1'}$
4142.9 (3800.7)	112 (42)	63	$\nu_{\text{O}_2\text{H}_2'}$
4146.9 (3771.1)	122 (104)	42	$\nu_{\text{O}_4\text{H}_4''}$ , $\nu_{\text{O}_4\text{H}_4'}$ (28.4%)
Ph-w <sub>4</sub> -4			
3814.1 (3064.2)	468 (815)	214	$\nu_{\text{OH}}$ , $\nu_{\text{O}_1\text{H}_1}$ (53.2%), $\nu_{\text{O}_2\text{H}_2}$ (21.8%)
3866.3 (3198.2)	1022 (1708)	24	$\nu_{\text{O}_2\text{H}_2}$ , $\nu_{\text{OH}}$ (77.3%), $\nu_{\text{O}_1\text{H}_1}$ (28.1%)
3899.5 (3270.9)	379 (760)	53	$\nu_{\text{O}_1\text{H}_1}$ , $\nu_{\text{O}_2\text{H}_2}$ (63.4%), $\nu_{\text{OH}}$ (12.0%)
3991.0 (3516.8)	225 (342)	54	$\nu_{\text{O}_3\text{H}_3'}$ , $\nu_{\text{O}_3\text{H}_3''}$ (23.8%)
4058.1 (3691.8)	27 (156)	38	$\nu_{\text{O}_4\text{H}_4'}$ , $\nu_{\text{O}_4\text{H}_4''}$ (69.6%)
4095.0 (3648.2)	218 (180)	53	$\nu_{\text{O}_3\text{H}_3''}$ , $\nu_{\text{O}_3\text{H}_3'}$ (25.5%)
4139.4 (3795.8)	114 (50)	85	$\nu_{\text{O}_1\text{H}_1'}$
4145.3 (3796.9)	89 (29)	61	$\nu_{\text{O}_2\text{H}_2'}$
4163.4 (3804.6)	79 (47)	29	$\nu_{\text{O}_4\text{H}_4''}$ , $\nu_{\text{O}_4\text{H}_4'}$ (62.2%)
Ph-w <sub>4</sub> -5			
3822.5	288	234	$\nu_{\text{OH}}$ , $\nu_{\text{O}_1\text{H}_1}$ (78.8%), $\nu_{\text{O}_2\text{H}_2}$ (46.2%)
3865.8	1227	7	$\nu_{\text{O}_2\text{H}_2}$ , $\nu_{\text{OH}}$ (73.5%)
3902.7	346	54	$\nu_{\text{O}_1\text{H}_1}$ , $\nu_{\text{O}_2\text{H}_2}$ (26.1%), $\nu_{\text{OH}}$ (17.1%)
3988.7	228	49	$\nu_{\text{O}_3\text{H}_3'}$ , $\nu_{\text{O}_3\text{H}_3''}$ (23.9%)
4060.3	19	28	$\nu_{\text{O}_4\text{H}_4}$ , $\nu_{\text{O}_4\text{H}_4''}$ (76.0%), $\nu_{\text{O}_3\text{H}_3''}$ (10.3%)
4090.7	229	58	$\nu_{\text{O}_3\text{H}_3''}$ , $\nu_{\text{O}_3\text{H}_3'}$ (26.6%)
4144.8	79	68	$\nu_{\text{O}_2\text{H}_2}$ , $\nu_{\text{O}_1\text{H}_1'}$ (56.8%)
4146.1	126	99	$\nu_{\text{O}_1\text{H}_1'}$ , $\nu_{\text{O}_2\text{H}_2'}$ (59.6%)
4163.5	69	25	$\nu_{\text{O}_4\text{H}_4'}$ , $\nu_{\text{O}_4\text{H}_4}$ (76.7%)
Ph-w <sub>4</sub> -6			
3815.7	534	211	$\nu_{\text{OH}}$
3866.0	906	59	$\nu_{\text{O}_2\text{H}_2}$
3972.1	514	110	$\nu_{\text{O}_3\text{H}_3}$
3992.4	145	108	$\nu_{\text{O}_4\text{H}_4}$ , $\nu_{\text{O}_1\text{H}_1''}$ (32.9%)
4007.3	190	27	$\nu_{\text{O}_1\text{H}_1''}$ , $\nu_{\text{O}_1\text{H}_1'}$ (48.3%), $\nu_{\text{O}_4\text{H}_4}$ (34.5%)
4088.7	252	45	$\nu_{\text{O}_1\text{H}_1'}$ , $\nu_{\text{O}_1\text{H}_1''}$ (33.3%)
4140.6	112	69	$\nu_{\text{O}_2\text{H}_2}$ , $\nu_{\text{O}_3\text{H}_3'}$ (12.4%)
4141.4	165	54	$\nu_{\text{O}_3\text{H}_3'}$ , $\nu_{\text{O}_2\text{H}_2'}$ (14.6%)
4154.8	128	60	$\nu_{\text{O}_4\text{H}_4'}$
Ph-w <sub>4</sub> -7			
3809.1	571	188	$\nu_{\text{OH}}$ , $\nu_{\text{O}_1\text{H}_1}$ (28.9%)
3869.4	894	46	$\nu_{\text{O}_2\text{H}_2}$ , $\nu_{\text{O}_1\text{H}_1}$ (68.2%), $\nu_{\text{OH}}$ (55.6%)
3905.6	440	51	$\nu_{\text{O}_1\text{H}_1}$ , $\nu_{\text{O}_2\text{H}_2}$ (84.0%)
3954.8	227	50	$\nu_{\text{O}_3\text{H}_3}$ , $\nu_{\text{O}_2\text{H}_2}$ (11.5%), $\nu_{\text{O}_4\text{H}_4}$ (11.4%)
3999.4	263	51	$\nu_{\text{O}_4\text{H}_4}$
4126.9	117	60	$\nu_{\text{O}_3\text{H}_3'}$
4143.1	111	95	$\nu_{\text{O}_1\text{H}_1'}$
4148.4	101	60	$\nu_{\text{O}_2\text{H}_2'}$
4155.5	126	42	$\nu_{\text{O}_4\text{H}_4'}$

TABLE 5 (Continued)

frequency	IR	Raman	assignment
Ph- <i>w</i> <sub>4</sub> -8			
3824.3	302	147	$\nu_{\text{O}_1\text{H}_1}, \nu_{\text{O}_2\text{H}_2}$ (26.6%)
3884.9	765	40	$\nu_{\text{O}_3\text{H}_3}, \nu_{\text{O}_2\text{H}_2}$ (83.4%), $\nu_{\text{O}_1\text{H}_1}$ (61.5%)
3919.1	434	46	$\nu_{\text{O}_3\text{H}_3}, \nu_{\text{O}_2\text{H}_2}$ (94.9%)
3977.9	334	63	$\nu_{\text{OH}}, \nu_{\text{O}_4\text{H}_4}$ (26.9%)
4003.4	300	90	$\nu_{\text{O}_4\text{H}_4}, \nu_{\text{OH}}$ (35.9%)
4131.9	202	39	$\nu_{\text{O}_4\text{H}_4'}, \nu_{\text{O}_1\text{H}_1}'$ (14.9%)
4135.9	81	91	$\nu_{\text{O}_1\text{H}_1}', \nu_{\text{O}_4\text{H}_4}'$ (11.0%)
4142.9	130	47	$\nu_{\text{O}_2\text{H}_2'}, \nu_{\text{O}_3\text{H}_3}$ (14.5%)
4144.4	84	83	$\nu_{\text{O}_3\text{H}_3'}, \nu_{\text{O}_2\text{H}_2}$ (16.1%)
Ph- <i>w</i> <sub>4</sub> -9			
3817.5	732	243	$\nu_{\text{OH}}, \nu_{\text{O}_1\text{H}_1}$ (33.8%)
3876.7	693	84	$\nu_{\text{O}_1\text{H}_1}, \nu_{\text{OH}}$ (94.2%), $\nu_{\text{O}_2\text{H}_2}$ (93.9%), $\nu_{\text{O}_3\text{H}_3}$ (34.2%)
3903.3	941	38	$\nu_{\text{O}_3\text{H}_3}, \nu_{\text{O}_1\text{H}_1}$ (81.5%), $\nu_{\text{O}_2\text{H}_2}$ (22.7%)
3932.0	302	60	$\nu_{\text{O}_2\text{H}_2}, \nu_{\text{O}_3\text{H}_3}$ (57.0%), $\nu_{\text{O}_1\text{H}_1}$ (15.3%)
3975.6	382	107	$\nu_{\text{O}_4\text{H}_4}, \nu_{\text{O}_3\text{H}_3}$ (11.6%)
4142.1	105	69	$\nu_{\text{O}_1\text{H}_1}'$
4146.2	116	67	$\nu_{\text{O}_4\text{H}_4'}, \nu_{\text{O}_3\text{H}_3}'$ (17.9%)
4146.6	128	27	$\nu_{\text{O}_3\text{H}_3'}, \nu_{\text{O}_2\text{H}_2}'$ (62.9%), $\nu_{\text{O}_4\text{H}_4}'$ (37.1%)
4147.5	118	74	$\nu_{\text{O}_2\text{H}_2'}, \nu_{\text{O}_3\text{H}_3}'$ (55.8%)

<sup>a</sup> Infrared intensity is in km/mol, Raman (R) activity in Å<sup>4</sup>/amu. The partial contributions are evaluated as the ratio of the total displacements. The contribution of the first reported mode is referred to 100%.

(symmetric) and 4146.9 (3771.1) (asymmetric) cm<sup>-1</sup>. Comparing with the  $\nu_1$  and  $\nu_3$  stretching vibrations of water molecule, the former is red shifted by 45 (180) cm<sup>-1</sup> whereas the latter is red shifted by 41 (144) cm<sup>-1</sup>.

The Ph-*w*<sub>4</sub>-4 structure also has a rather peculiar and non-separable OH stretching vibrational pattern. Its three most red-shifted vibrations are located at 3814 (3064.2), 3866 (3198.2), and 3900 (3270.9) cm<sup>-1</sup>. Altogether, they describe the coupled OH stretching vibrations of the trimeric water ring and the phenolic OH-group. The second one is the most IR active among all OH stretching vibrations of all reported Ph-*w*<sub>4</sub> structures. Its IR intensity is in 13 (18) times larger that of the OH stretching vibration of bare phenol ( $\nu_3$  of water molecule). The symmetric and asymmetric stretches of the water molecule connecting the water ring with the terminated water molecule placed above the phenol ring are found at 3991 (3516.8) and 4095 (3648.2) cm<sup>-1</sup>. Between them, at 4058 (3691.8) cm<sup>-1</sup>, there exists the symmetric  $\pi$  OH stretch whose asymmetric vibration has the highest frequency of 4163 (3804.6) cm<sup>-1</sup>. These two vibrations are separated by the OH stretches at 4139 (3795.8) and 4145 (3796.9) cm<sup>-1</sup> assigned to free OH-groups of water molecules.

As we expect, the pattern of the OH stretching vibrations of Ph-*w*<sub>4</sub>-1 is absolutely different from those of Ph-*w*<sub>4</sub>-2, Ph-*w*<sub>4</sub>-3, and Ph-*w*<sub>4</sub>-4 and resembles the typical S<sub>4</sub> pattern of the Ph-*w*<sub>1</sub>, Ph-*w*<sub>2</sub>, and Ph-*w*<sub>3</sub>-1–4 structures. It is clearly seen from Table 5 that the nine OH stretching vibrations of the Ph-*w*<sub>4</sub>-1 structure are well separated into two groups forming in that way a “window” region of about 164 (327) cm<sup>-1</sup> in width. Notice that the B3LYP/A width satisfactorily agrees with the experimental one.<sup>6d</sup> The former group spans the region between 3812 (3077.8; exptl  $\approx$  3135<sup>6d</sup>) and 3977 (3468.8; exptl  $\approx$  3430<sup>6d</sup>) cm<sup>-1</sup> and consists of five rather IR and Raman active OH stretching vibrations assigned to the coupled stretches of the water ring and phenolic OH-groups. Its highest OH stretching vibration is dominantly composed of the H stretch of the water molecule donating the hydrogen bond to phenol. The latter group is rather narrow with the width of only 4 (4) cm<sup>-1</sup>. The OH stretching vibrations of free water OH-groups contribute to this group. Its lowest wavenumber stretch at 4141 (3796.0) cm<sup>-1</sup> corresponds to the free OH-group of the water molecule which accepts the phenolic H-bond.

Summarizing the B3LYP/A IR patterns in the stretching region of the four most energetically stable structures Ph-*w*<sub>4</sub>-1, Ph-*w*<sub>4</sub>-2, Ph-*w*<sub>4</sub>-3, and Ph-*w*<sub>4</sub>-4 leads us to the following conclusion: the “window” region of the Ph-*w*<sub>4</sub>-1 structure spreads from 3468.8 to 3796.0 cm<sup>-1</sup> and is 327 cm<sup>-1</sup> wide (the experimental value is 281 cm<sup>-1</sup><sup>6d</sup>). As follows from Table 5, in this region, the isomer Ph-*w*<sub>4</sub>-4 has four OH stretching modes placed at 3516.8, 3648.2, 3691.8, and 3795.8 cm<sup>-1</sup>. Ph-*w*<sub>4</sub>-3 also has four OH stretching modes there, viz., 3593.9, 3670.3, 3771.1, and 3792.2 cm<sup>-1</sup>, whereas Ph-*w*<sub>4</sub>-2 possesses five modes there: 3476.8, 3515.8, 3721.9, 3763.5, and 3794.8 cm<sup>-1</sup>. In the other words, the Ph-*w*<sub>4</sub>-3 and Ph-*w*<sub>4</sub>-4 have precisely that number of the vibrational modes which was revealed experimentally.<sup>6c–d</sup> Due to theoretical and experimental uncertainties, the structure Ph-*w*<sub>4</sub>-2 can be also included in this class. Therefore, these three lower energy structures of phenol with four water molecules characterized by the formation of the  $\pi$  hydrogen bond are likely referred to the class of the structures revealed by Stanley and Castleman.<sup>7a</sup> It is worth mentioning that the lowest stretching mode of the nonring structure of Ph-(H<sub>2</sub>O)<sub>4</sub> is observed to be placed by 73 cm<sup>-1</sup> below the analogous one in the ring S<sub>4</sub> structure Ph-*w*<sub>4</sub>-1.<sup>6d</sup> As follows then from Table 5, Ph-*w*<sub>4</sub>-2 and Ph-*w*<sub>4</sub>-3 have a similar feature, viz., 108 and 69 cm<sup>-1</sup>, respectively.

#### 4. Summary and Conclusions

As we have already mentioned in Introduction, the past decade was unprecedentedly successful, primarily from the experimental point of view, in studying the interaction between phenol and water molecules. It was particularly discovered that phenol favors a two-dimensional ring type of arrangements of water molecules if they are less than *three* and, on the contrary, the three-dimensional one if they are equal to and more than *five*. It was therefore thought that *four* looks like a “magic” number for the phenol–water<sub>*n*</sub> interaction. And this was really a sort of exclusive number thanks, first of all, to the experimental works by Stanley and Castleman group and those by the Mikami and Ebata group who experimentally revealed the existence of the phenol–water<sub>4</sub> isomer with three-dimensional arrangement of water molecules and showed that it was only that isomer which is capable to explain the puzzled “window” region in



the IR stretching spectra. Logically, a “magic” of the number four stems out from the fact that this is just the borderline where two-dimensional water pattern ( $n \leq 3$ ) meets the three-dimensional one ( $n \geq 5$ ). The thorough analysis of the potential energy surface of the phenol–water<sub>4</sub> complex, conducted in the present work and juxtaposing it with the PESs of the phenol–water<sub>1–3</sub> complexes, vividly demonstrates that viewpoint by revealing four different structures residing near its global minimum which have either two-dimensional or three-dimensional patterns of water molecules and which, altogether, provide a full explanation of the origin of the puzzled “window” region in the stretching part of IR spectra. A three-dimensional pattern originates when the terminated water molecule becomes contiguous to the  $\pi$  cloud of the phenol ring. In terms of the theory of hydrogen bonding,<sup>19</sup> this fact can be explained by that the ability of the phenolic OH-group to accept a hydrogen bond becomes almost exhausted when three water molecules form a two-dimensional ring nearby it (similarly to the ring or book structures of water hexamer which are no longer energetically favorable<sup>11</sup>) and, therefore, competes with the ability of the  $\pi$  cloud of the phenol ring to form the subtle  $\pi$  one with a water molecule.

**Acknowledgment.** E.S.K. gratefully acknowledges the Grant S-99096 of the Japan Society for the Promotion of Science. He deeply thanks Georg Zundel for many inspiring and helpful discussions during the last 15 years and Thérèse Zeegers-Huyskens and Minh Tho Nguyen for useful discussions and warm hospitality during his work in Leuven where this work has been completed. We thank the referees for valuable comments and suggestions.

## References and Notes

- (1) (a) Abe, H.; Mikami, N.; Ito, M. *J. Phys. Chem.* **1982**, *86*, 1768. (b) Fuke, K.; Kaya, K. *Chem. Phys. Lett.* **1983**, *94*, 97. (c) Oikawa, A.; Abe, H.; Mikami, N.; Ito, M. *J. Phys. Chem.* **1983**, *87*, 5083. (d) Goto, A.; Fujii, M.; Mikami, N.; Ito, M. *J. Phys. Chem.* **1986**, *90*, 2370.
- (2) (a) Lipert, R. J.; Colson, S. D. *Chem. Phys. Lett.* **1989**, *161*, 303. (b) Lipert, R. J.; Colson, S. D. *J. Chem. Phys.* **1988**, *89*, 4579. (c) Lipert, R. J.; Colson, S. D. *J. Phys. Chem.* **1989**, *93*, 135, 3894. (d) Lipert, R. J.; Colson, S. D. *J. Phys. Chem.* **1990**, *94*, 2358. (e) Lipert, R. J.; Bermudez, G.; Colson, S. D. *J. Phys. Chem.* **1988**, *92*, 3801.
- (3) Hartland, G. V.; Henson, B. F.; Venturo, V. A.; Felker, P. M. *J. Phys. Chem.* **1992**, *96*, 1164.
- (4) (a) Schmitt, M.; Mueller, H.; Kleinermanns, K. *Chem. Phys. Lett.* **1994**, *218*, 246. (b) Gerhards, M.; Beckmann, K.; Kleinermanns, K. *Z. Phys. D* **1994**, *29*, 223. (c) Gerhards, M.; Kleinermanns, K. *J. Chem. Phys.* **1995**, *103*, 7392. (d) Jacoby, Ch.; Roth, W.; Schmitt, M.; Janzen, Ch.; Spangenberg, D.; Kleinermanns, K. *J. Phys. Chem. A* **1998**, *102*, 4471. (e) Berden, G.; Meerts, W. L.; Schmitt, M.; Kleinermanns, K. *J. Chem. Phys.* **1996**, *104*, 972.
- (5) (a) Gerhards, M.; Schmitt, M.; Kleinermanns, K.; Stahl, K. *J. Chem. Phys.* **1996**, *104*, 967. (b) Kleinermanns, K.; Gerhards, M.; Schmitt, M. *Ber. Bunsen-Ges. Phys. Chem.* **1997**, *101*, 1785. (c) Schmitt, M.; Jacoby, Ch.; Kleinermanns, K. *J. Chem. Phys.* **1998**, *108*, 4486. (d) Roth, W.; Schmitt, M.; Jacoby, Ch.; Spangenberg, D.; Janzen, Ch.; Kleinermanns, K. *Chem. Phys.* **1998**, *239*, 1.
- (6) (a) Ebata, T.; Furukawa, M.; Suzuki, T.; Ito, M. *J. Opt. Soc. Am. B* **1990**, *7*, 1890. (b) Tanabe, S.; Ebata, T.; Fujii, M.; Mikami, N. *Chem. Phys. Lett.* **1993**, *215*, 347. (c) Mikami, N. *Bull. Chem. Soc. Jpn.* **1995**, *68*, 683. (d) Watanabe, T.; Ebata, T.; Tanabe, S.; Mikami, N. *J. Chem. Phys.* **1996**, *105*, 408. (e) Fujii, A.; Sawamura, T.; Tanabe, S.; Ebata, T.; Mikami, N. *Chem. Phys. Lett.* **1994**, *225*, 104. (f) Ebata, T.; Fujii, A.; Mikami, N. *Int. Rev. Phys. Chem.* **1998**, *17*, 331.
- (7) (a) Stanley, R. J.; Castleman, A. W., Jr. *J. Chem. Phys.* **1991**, *94*, 7744. (b) Stanley, R. J.; Castleman, A. W., Jr. *J. Chem. Phys.* **1993**, *98*, 796.
- (8) (a) Schütz, M.; Bürgi, T.; Leutwyler, S.; Fischer, T. *J. Chem. Phys.* **1993**, *98*, 3763. (b) Schütz, M.; Bürgi, T.; Leutwyler, S. *J. Mol. Struct. (THEOCHEM)* **1992**, *276*, 117. (c) Schütz, M.; Bürgi, T.; Leutwyler, S.; Bürgi, H. B. *J. Chem. Phys.* **1993**, *99*, 5228. (d) Leutwyler, S.; Bürgi, T.; Schütz, M.; Taylor, A. *Faraday Discuss. Chem. Soc.* **1994**, *96*. (e) Bürgi, T.; Schütz, M.; Leutwyler, S. *J. Chem. Phys.* **1995**, *103*, 6350.
- (9) (a) Dopfer, O.; Müller-Dethlefs, K. *J. Chem. Phys.* **1994**, *101*, 8508. (b) Helm, R. M.; Neusser, H. *J. Chem. Phys.* **1998**, *239*, 33. (c) Barth, H.-D.; Buchhold, K.; Djafari, S.; Reimann, B.; Lommatzsch, U.; Brutschy, B. *J. Chem. Phys.* **1998**, *239*, 49. (d) Helm, R. M.; Vogel, H.-P.; Neusser, N. *J. Chem. Phys.* **1998**, *108*, 4496. (e) Neusser, H. J.; Siglow, K. *Chem. Rev.* **2000**, *100*, 3921. (f) Dessent, C. E. H.; Müller-Dethlefs, K. *Chem. Rev.* **2000**, *100*, 3999.
- (10) (a) Schlag, E. W. In *Advances in Chemical Physics, Volume 101: Chemical Reactions and Their Control on the Femtosecond Time Scale, XXth Solvay Conference on Chemistry*; Gaspard, P., Burghardt, I., Prigogine, I., Rice, S. A., Eds.; Wiley: New York, 1997; pp 607–623. (b) Courty, A.; Mons, M.; Dimicoli, I.; Piuze, F.; Brenner, V.; Millié, P. *J. Phys. Chem. A* **1998**, *102*, 4890. (c) Syage, J. A. *J. Phys. Chem.* **1995**, *99*, 5772.
- (11) (a) Kim, K.; Jordan, K. D.; Zwier, T. S. *J. Am. Chem. Soc.* **1994**, *116*, 11568. (b) Liti, K.; Brown, M. G.; Carter, C.; Saykally, R. J.; Gregory, J. K.; Clary, D. C. *Nature* **1996**, *501*. (c) Kryachko, E. S. *Int. J. Quantum Chem.* **1998**, *70*, 831. (d) Kryachko, E. S. *Chem. Phys. Lett.* **1999**, *314*, 353 and references therein.
- (12) Feller, D.; Feyereisen, M. W. *J. Comput. Chem.* **1993**, *14*, 1027.
- (13) (a) Benoit, D. M.; Chavagnac, A. X.; Clary, D. C. *Chem. Phys. Lett.* **1998**, *283*, 269. (b) Benoit, D. M.; Clary, D. C. *J. Phys. Chem. A* **2000**, *104*, 5590. (c) Clary, D. C.; Benoit, D. M.; Van Mourik, T. *Acc. Chem. Res.* **2000**, *33*, 441.
- (14) Fang, W. *J. Chem. Phys.* **2000**, *112*, 1204.
- (15) (a) Sodupe, M.; Oliva, A.; Bertrán, J. *J. Phys. Chem. A* **1997**, *101*, 9142. (b) Guedes, R. C.; Costa Cabral, B. J.; Martinho Simões, J. A.; Diogo, H. P. *J. Phys. Chem. A* **2000**, *104*, 6062. (c) Re, S.; Osamura, Y. *J. Phys. Chem. A* **1998**, *102*, 3798.
- (16) Fang, W.-H.; Liu, R.-Z. *J. Chem. Phys.* **2000**, *113*, 5253.
- (17) (a) Watanabe, H.; Iwata, S. *J. Chem. Phys.* **1996**, *105*, 420. (b) Watanabe, H.; Iwata, S. *Int. J. Quantum Chem., Quantum Chem. Symp.* **1996**, *30*, 395.
- (18) Kryachko, E. S.; Nguyen, M. T. *J. Chem. Phys.* **2001**, *114*, 0000.
- (19) Schuster, P.; Zundel, G.; Sandorfy, C., Eds. *The Hydrogen Bond. Recent Developments in Theory and Experiments*; North-Holland: Amsterdam, 1976. Also see: Zundel, G. *Adv. Chem. Phys.* **2000**, *111*, 1 and references therein.
- (20) (a) Bačić, Z.; Miller, R. E. *J. Phys. Chem.* **1996**, *100*, 12945. (b) Kim, K. S.; Lee, J. L.; Choi, H. S.; Kim, J.; Jang, J. H. *Chem. Phys. Lett.* **1997**, *265*, 497. (c) Kim, K. S.; Tarakeshwar, P.; Lee, J. Y. *Chem. Rev.* **2000**, *100*, 4145.
- (21) Hehre, W. J.; Radom, L.; Schleyer, P. v. R.; Pople, J. A. *Ab Initio Molecular Orbital Theory*; Wiley: New York, 1986.
- (22) Frisch, M. J.; Trucks, G. W.; Schlegel, H. B.; Scuseria, G. E.; Robb, M. A.; Cheeseman, J. R.; Zakrzewski, V. G.; Montgomery, Jr., J. A.; Stratmann, R. E.; Burant, J. C.; Dapprich, S.; Millam, J. M.; Daniels, A. D.; Kudin, K. N.; Strain, M. C.; Farkas, O.; Tomasi, J.; Barone, V.; Cossi, M.; Cammi, R.; Mennucci, B.; Pomelli, C.; Adamo, C.; Clifford, S.; Ochterski, J.; Petersson, G. A.; Ayala, P. Y.; Cui, Q.; Morokuma, K.; Malick, D. K.; Rabuck, A. D.; Raghavachari, K.; Foresman, J. B.; Cioslowski, J.; Ortiz, J. V.; Stefanov, B. B.; Liu, G.; Liashenko, A.; Piskorz, P.; Komaromi, I.; Gomperts, R.; Martin, R. L.; Fox, D. J.; Keith, T.; Al-Laham, M. A.; Peng, C. Y.; Nanayakkara, A.; Gonzalez, C.; Challacombe, M.; Gill, P. M. W.; Johnson, B.; Chen, W.; Wong, M. W.; Andres, J. L.; Head-Gordon, M.; Replogle, E. S.; Pople, J. A. *GAUSSIAN 98*, revision A.5; Gaussian, Inc.: Pittsburgh, PA, 1998.
- (23) (a) Michalska, D.; Bieńko, D. C.; Abkowitz-Bieńko, A. J.; Latajka, Z. *J. Phys. Chem.* **1996**, *100*, 17768. (b) Lampert, H.; Mikenda, W.; Karpfen, A. *J. Phys. Chem. A* **1997**, *101*, 2254. (c) Keresztury, G.; Billes, F.; Kubinyi, M.; Sundius, T. *J. Phys. Chem. A* **1998**, *102*, 1371.
- (24) Flaud, J. M.; Camy-Payret, C.; Maillard, J. P. *Mol. Phys.* **1976**, *32*, 499.